WEAVER, ALLISON DEAL, M.S. Temporal Expression of Nitric Oxide Synthase in *Ilyanassa obsoleta* Using an *Ilyanassa*-Specific NOS Antibody. (2009)
Directed by Dr. Mark D. Hens and Dr. Esther M. Leise. 71pp.

In the mollusc *Ilyanassa obsoleta*, metamorphosis is a key event in its life history that is closely regulated by positive and negative modulators. Previous research has determined that nitric oxide (NO) and nitric oxide synthase (NOS) maintain the larval state up to competency. RT-PCR of NOS transcripts, NADPH-diaphorase staining, and immunohistochemistry have all confirmed the presence of NOS during larval development and metamorphosis. However, these assays have given conflicting results on when and where NOS is produced. I developed an *Ilyanassa*-specific NOS antibody that was used in western blot analysis of larval extracts to determine temporal expression of the NOS protein. *In situ* hybridization was also done to localize NOS transcripts. My *Ilyanassa*-specific antibody recognized NOS, but the most prominently recognized epitope, a 66 kDa polypeptide, is likely to be a degradation product of NOS. *In situ* hybridization on competent larvae provided no meaningful data. My studies of temporal expression of the protein confirmed the previous RT-PCR results which demonstrated a constant level of NOS during larval development and a decrease in NOS during metamorphosis. These results were unlike those of previous NADPH-diaphorase histochemistry and suggest regulation of NOS enzymatic activity. My results indicate that metamorphosis in *Ilyanassa* may be controlled by the regulation of the quantity of NOS present as well as regulation of the level of NOS enzymatic activity.

TEMPORAL EXPRESSION OF NITRIC OXIDE SYNTHASE IN *ILYANASSA OBSOLETA* USING AN *ILYANASSA*-SPECIFIC NOS ANTIBODY

by

Allison Deal Weaver

A Thesis Submitted to
The Faculty of The Graduate School at
The University of North Carolina at Greensboro
in Partial Fulfillment
of the Requirements of the Degree
Master of Science

Greensboro
2009

Approved by

_____
Committee Co-Chair

_____
Committee Co-Chair

APPROVAL PAGE

This thesis has been approved by the following committee of the Faculty of The Graduate School at The University of North Carolina at Greensboro.

Committee Co-Chair_____

Committee Co-Chair_____

Committee Members_____

_____

_____
Date of Acceptance by Committee

_____
Date of Final Oral Examination

TABLE OF CONTENTS

Page

LIST OF FIGURES

Page

CHAPTER I

INTRODUCTION

Molluscs, members of the second largest phylum of animals, are found both on land and in aquatic environments and are important as model organisms for the study of neurobiology and evolutionary biology (Haszprunar, 2002). The life histories of molluscs vary and are greatly dictated by the environment in which a species lives. After fertilization, embryos usually undergo spiral cleavage and commonly develop into free swimming larvae (Anderson, 2001). Free swimming larvae may be planktotrophic, meaning they eat other organisms, or they may be lecithotropic, which means the larvae live off of yolk supplements from the egg (Boxshall, 2007).

In marine snails, such as *Ilyanassa obsoleta*, development consists of a free-swimming planktonic larval stage followed by metamorphosis to a benthic adult form (Pawlik, 1992). Larval morphology differs from that of the adult and free swimming larvae may travel many miles in search of a suitable substrate on which to settle (Pawlik, 1992; Scheltma, 1961). Because it is critical that a suitable substrate is located before metamorphosis occurs, chemical cues in the environment may direct larvae towards a favorable juvenile habitat.

Metamorphosis in molluscs

Although the exact chemicals involved in the triggering of metamorphosis in molluscs have been difficult to identify, a number of compounds have been implicated in the settlement and metamorphosis of planktonic larvae. Chemicals that induce settlement, the behavioral cessation of swimming, and metamorphosis vary by species of mollusc and in some cases multiple compounds have been identified that trigger these behaviors (Yu *et al*., 2008). Some molluscan species exhibit settlement or metamorphosis in response to chemicals associated with potential prey or conspecifics (Morse *et al*., 1984; Leise *et al*., 2009; Zimmer-Faust and Tamburri, 1994). For example, soluble products released by the prey coral species, *Porites compressa*, cause *Phestilla sibogae*, a marine slug, to metamorphose (Hadfield, 1998; Pires *et al*., 2000). The scallop, *Pecten maximus,* settles in the presence of jacaranone, a chemical found in a species of red alga (Yvin *et al*., 1985). For the red abalone, *Haliotis rufescens*, a compound on the surface of its prey, a crustose red alga, triggers metamorphosis (Morse *et al*., 1984). An example of conspecific-triggered behavior is in the species *Crassostrea viginica,* in which adults produce a low-molecular weight peptide that causes larvae to settle (Zimmer-Faust and Tamburri, 1994).

In other species, neurotransmitters can trigger metamorphosis, for example, serotonin induces metamorphosis in *Ilyanassa obsoleta* and settlement in *Pinctada fucata martensii* (Levantine and Bonar, 1986; Yu *et al*., 2008). Other neurotransmitters, such as γ-aminobutyric acid (GABA), induce larvae of *Haliotis rufescens* to settle and begin

metamorphosis, but for these abalone, GABA is mimicking an algal ligand and is not acting as an internal neurotransmitter (Morse, 1979).

Metamorphosis in *Ilyanassa obsoleta*

Ilyanassa obsoleta is a mollusc whose metamorphic cues are still being investigated. Both internal and external changes occur during metamorphosis in *Ilyanassa.* Larvae that emerge from egg capsules are about 250µm long (Scheltema, 1962) and they are identifiable by two ciliated velar lobes with which they swim and catch single-celled algae. Larvae grow to about 600µm in shell length, at which point they are competent, or capable of metamorphosing. Larvae usually reach this size seventeen to twenty-one days after hatching, although size, rather than age seems to be a better indicator of competence (Leise *et al.*, 2004). Upon induction of metamorphosis, ciliated cells begin to fall off of the velar lobes and eventually both velar lobes are completely shed (Scheltema, 1962; Couper and Leise, 1996). The velar lobes are typically lost within thirty-six hours of induction of metamorphosis (Scheltema, 1962; Leise *et al.*, 2004; Lin and Leise 1996a). The major part of the metamorphic process is usually complete by forty-eight hours after experimental induction of metamorphosis with serotonin (5-HT) (Levantine and Bonar, 1986; Couper and Leise, 1996).

Along with external changes, notable internal neuroanatomical modifications occur. During larval development, key adult structures emerge, including intestinal ganglia, paired buccal, pleural, and cerebral ganglia and an anterodorsal apical ganglion (Lin and Leise, 1996a). The apical ganglion (AG), or apical sensory organ, contains both

serotonergic and nitrergic neurons and innervates the velar lobes (Leise *et al.*, 2001; Leise *et al.*, 2004; Dickenson and Croll, 2003). All ganglia, including the AG, can be seen in the central nervous system by 83% of larval development. During metamorphosis, the AG disappears by a form of programmed cell death (Gifondorwa and Leise, 2006; Lin and Leise, 1996b). Because the disappearance of the AG is central to the process of metamorphosis, we need to understand the moleculer mechanisms that maintain or cause the disappearance of this structure.

Pharmacology of metamorphosis in molluscs

For some molluscs, the molecular mechanisms that mediate settlement and metamorphosis are being unraveled. As stated earlier, larval *Haliotis rufescens* are induced to metamorphose by GABA which is thought to mimick a GABA-like compound on the surface of red algae (Morse *et al*., 1984; Morse, 1979). For *H. rufescnens*, both GABA and the algal inducer appear to bind to the same chemoreceptors (Trapido-Rosenthal and Morse, 1986). The binding of GABA to the epithelium may cause an efflux of chloride ions thereby depolarizing the chemosensory neurons (Morse, 1979; Morse, 1985; Trapido-Rosenthal and Morse, 1986).

In most larvae, there is not such a clear connection between natural inducers and their molecular effects. In *Phestilla sibogae*, endogenous catecholamines increase as the larval slug reaches competence (Pires *et al*., 2000). The increase in catecholamines can be triggered by bath application of L-Dopa, a precursor to the catecholamine dopamine, but metamorphosis can only be triggered by *P. sibogae's* coral prey (Pires *et al*., 2000).

For *Ilyanassa obsoleta*, a centric diatom, *Coscinodisus sp*., can induce metamorphosis but the chemical composition of the inductive molecule is unknown (Leise *et al*., 2009). Serotonin, which is commonly used to induce metamorphosis in *Ilyanassa* in the laboratory, acts internally in the larva as a neurotransmitter, as opposed to the external action of a GABA-like environmental inducer (Levantine and Bonar, 1986; Couper and Leise, 1996). When fluoxetine, a 5-HT reuptake inhibitor, was injected into competent larvae, levels of metamorphosis increased, whereas when 5-HT was injected along with a 5-HT antagonist, gramine, levels of metamorphosis decreased (Couper and Leise, 1996).

As with most developmental processes, there is both negative and positive regulation of metamorphosis. In molluscs, there are chemicals that control the onset of metamorphosis as well as those that maintain the larval state until competency. Molecules such as the free radical, nitric oxide, have been shown to maintain the larval state in *Ilyanassa* (Froggett and Leise, 1999). Timely inhibition of metamorphosis allows larval *Ilyanassa* to find appropriate environmental conditions before undergoing metamorphosis.

Nitric oxide is a common inhibitor of metamorphosis in other invertebrate species as well. In both the sea urchin, *Lytechinus pictus,* and the slippershell snail, *Crepidula fornicata,* nitric oxide inhibits metamorphosis (Bishop and Brandhorst, 2001; Pechenick *et al*., 2007). In the tunicates *Ciona intestinalis*, *Cnemidocarpa finmarkiensis* and *Boltenia villosa*, nitric oxide inhibits tail reabsorption, a key indicator of metamorphosis in these species (Bishop *et al*., 2001; Comes *et al*., 2007).

The role of nitric oxide in metamorphosis

Nitric oxide (NO) is a widely recognized neurotransmitter and neuromodulator that is highly reactive and diffuses easily through membranes (Palumbo, 2005). Three members of the nitric oxide synthase (NOS) gene family have been identified in mammals, including neuronal NOS, inducible NOS and endothelial NOS, but each type can be expressed in a variety of tissue types (Dawson and Synder, 1994). NO has been widely studied because of its ability to activate guanylyl cyclase which in turn produces cyclic GMP (Jacklet, 1997). Neuronal NO is produced on demand by the conversion of L-arginine to nitric oxide and citrulline by neuronal nitric oxide synthase (nNOS). Cyclic GMP has been implicated in such processes as ion channel regulation, vasodilation and apoptosis (Jacklet, 1997).

The molecular weight of human NOS is between 130-160kDa, depending on the isoform (Jacklet, 1997; Alderton *et al*., 2001). Neuronal NOS has binding sites for calmodulin (CaM), flavin mononucleotide (FMN), flavin adenine dinucleotide (FAD) and nicotinamide adenine dinucleotide phosphate (NADPH) (Figure 1) (Regulski and Tully, 1995). All types of NOS require calcium-calmodulin binding to induce enzymatic activity. Inducible NOS has a much lower requirement for calcium than the other types because CaM binds to iNOS independantly of calcium. (Jacklet, 1997; Alderton *et al*., 2001)

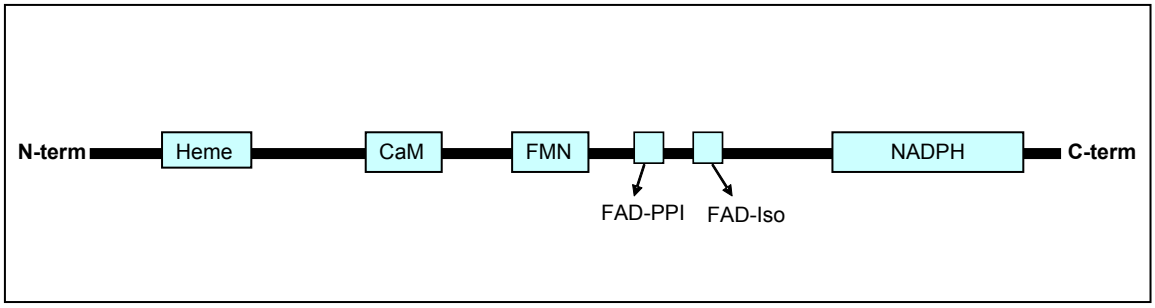

Figure 1. Schematic diagram of neuronal NOS. NOS is usually 130-160 kDa in size and contains distinct regulatory domains for several cofactors: Heme, CaM, FMN, FAD and NADPH. These cofactors are essential for its enzymatic funtion.

Comparisons of molluscan (*Lymnaea stagnalis*) and rat NOS orthologs demonstrate approximately 50% similarity at the amino acid level, indicating that the protein emerged early in metazoan evolution (Korneev *et al*., 1997). The portion of the nitric oxide synthase protein in *Ilyanassa obsoleta* that contains the calcium-calmodulin binding domain is highly conserved and demonstrates 70% similarity to human neuronal NOS and 71% similarity to rat neuronal NOS (Hens *et al*., 2006). Compared to neuronal NOS of other molluscs, the calcium-calmodulin binding domain of *Ilyanassa* is 94% similar to *Aplysia californica* and 91% similar to that of *Lymnaea stagnalis* (Hens *et al*., 2006.) Because of its conserved nature, I targeted this region for my creation of *Ilyanassa*-specific probes. The compete nucleotide sequence of NOS from *Ilyanassa* is not available and therefore the protein can not be compared to mammalian or molluscan species.

Nitric oxide function varies among molluscan species. In the snail, *Lymnaea stagnalis,* NO intitiates feeding behavior (Korneev and Shea, 2002) and in the slug, *Limax maximus,* NO is involved in the olfactory recognition of prey (Gelperin *et al.*,

2000). In *Mytilus galloprovincialis*, nitric oxide is produced by hemocytes as part of the immune response (Novas *et al*., 2007). In several molluscs, NO has been implicated in the negative regulation of metamorphosis (Froggett and Leise, 1999; Pechenick *et al*., 2007).

In *Ilyanassa obsoleta,* NO represses the onset of metamorphosis. Lin and Leise (1996b) used NADPH-diaphorase (NADPHd) histochemistry (Hope *et al.*, 1991; Dawson *et al.*, 1991) to show the presence of nitric oxide synthase in the neuropil (dendritic or axonal projections) of the AG of *Ilyanassa obsoleta*. NADPHd staining in the AG increases during larval development but sharply decreases upon induction of metamorphosis with serotonin. This suggested that NOS and NO might play a key role in the regulation of metamorphosis (Lin and Leise, 1996b).

The putatitive inhibitory role of NO in metamorphosis was further demonstrated by Froggett and Leise (1999) by treatment of larval *Ilyanassa* with NO-donors. In this study, larvae were treated with the NO-donors, S-nitroso-N-acetyl-D, L-Penicillamine (SNAP) and 3-morpholino-sydnonimine (SIN-1). When larvae were treated with a NO-donor alone, levels of metamorphosis were similar to those of the control group. When larvae were treated with both serotonin and a NO donor at high concentrations, levels of metamorphosis decreased as compared to metamorphic induction with only serotonin (Froggett and Leise, 1999). In addition, NOS inhibitors, such as N-nitro-L-arginine methyl ester (L-NAME) or N-methyl-L-arginine acetate (L-NMMA) induced significant levels of metamorphosis when injected into larvae in the absence of serotonin (Froggett and Leise, 1999). Unlike these inhibitors, 7-nitroindazole (Ni-7), a newer NOS inhibitor,

induces metamorphosis in bath application (Gifondorwa and Leise, 2006). These experiments provided considerable evidence for an inhibitory role for NO in the metamorphic process.

Gifondorwa and Leise (2006) suggest that decreases in NOS activity in the AG and the total loss of the AG during metamorphosis are due to programmed cell death. NO can inhibit DNA synthesis and thus inhibit programmed cell death by slowing the cell cycle (Peunova *et al.*, 1996). DNA fragmentation, a major characteristic of the early part of programmed cell death that is detected by terminal deoxynucleotidyl transferase dUTP Nick End Labeling (TUNEL), was observed in metamorphosing larvae after 7-Ni induction (Gifondorwa and Leise, 2006). This suggests that NO inhibits programmed cell death in the AG, thereby preventing metamorphosis until the larva encounters appropriate environmental conditions.

More direct attempts at demonstrating the presence of NOS in *Ilyanassa* have shown somewhat contradictory results. To localize NOS in the cell bodies of the AG, Thavaradhara and Leise (2001) treated larvae collected during different stages of development with a mammalian NOS antibody. Whole mount preparations of larvae were examined for NOS-like immunoreactivity (Thavardhara and Leise, 2001). Immunoreactivity was seen in the cell bodies of the AG and the number of immunoreactive cells increased as larvae grew; larvae had the greatest number of immunoreactive cells at competence (Thavardahara and Leise, 2001). Although NOS immunoreactivity was detected, the results are somewhat contradictory compared to results of the NADPHd staining. NOS is a form of NADPH-diaphorase, so this

histochemical method has become a traditional means by which NOS activity can be detected (Hope *et al*., 1991). Results of NADPHd staining had indicated that NOS activity was present in the neuropil of the AG while NOS-like immunoreactivity was visualized only in its cell bodies. The meaning of these differences is still unclear.

To further investigate the expression of neuronal NOS in larval *Ilyanassa*, mRNA levels were measured directly. In experiments done by Hens *et al*.(2006), mRNA was isolated from developing and metamorphosing larvae. Larvae that were collected following bath application of 5-HT showed a detectable decrease in NOS mRNA levels as early as two hours after induction (Hens *et al*., 2006). In contrast, larvae that were cultured in the absence of 5-HT and collected during different stages of development showed no difference in levels of NOS transcripts. These results confirm the presence of NOS mRNA during larval development and suggest that the decrease in NOS activity and resulting programmed cell death caused by 5-HT induction is due to the decreasing levels of NOS mRNA (Hens *et al.*, 2006).

To further characterize neuronal nitric oxide synthase in larval *Ilyanassa obsoleta,* I developed an *Ilyanassa*-specific NOS antibody. I characterized the antibody and used it to determine temporal patterns of nitric oxide synthase expression in both developing and metamorphosing larvae. Also, to further investigate the location of NOS transcripts, I performed *in situ* hybridization on larval *Ilyanassa.*

Hypothesis and specific aims

The hypothesis guiding my research was that metamorphosis in *Ilyanassa obsoleta* can only proceed with a decrease in nitric oxide levels, which is caused by a decrease in nitric oxide synthase activity in the AG. This hypothesis was tested by the following objectives.

Aim 1: Generate *Ilyanassa obsoleta*-specific NOS antibodies.

Aim2: Determine temporal expression nitric oxide synthase in the central nervous system of developing and metamorphosing larvae using the antibodies generated in aim 1.

Aim 3: Localize nitric oxide gene expression in *Ilyanassa obsoleta*.

CHAPTER II

METHODS

Animal care and maintenance

Adult *Ilyanassa obsoleta* (Say,1822) were collected between the months of December and March of 2005 to 2007 from the mudflats of the University of North Carolina at Wilmington Center for Marine Science in Wilmington, North Carolina. Adults were maintained at approximately 26ºC in 20 gal aquaria in Instant Ocean and fed frozen fish every other day. Additional adults were collected in March 2006 and maintained at 6ºC in 20 gal aquaria also in Instant Ocean. These adults remained unfed until they were needed and were then transferred to aquaria at 26ºC to induce egg laying.

Egg capsules were collected from the walls of the aquaria as needed and available. Approximately 350-450 egg capsules were collected at a time and washed in a nitex mesh filter in 70% ethanol and then with 0.22µm filtered Instant Ocean (FIO). Clean egg capsules were transferred to finger bowls containing fresh FIO.

Hatched larvae were removed daily from the finger bowls and the remaining egg capsules were washed as above. Hatched larvae were placed in about 650 ml of culture solution containing approximately 700 larvae in larval seawater (half 0.22µm filtered seawater and half FIO). Cultures were maintained by placing larvae in an airlift system consisting of a 400 ml plastic tripour beaker fitted with a 130µm nitex mesh filter on its bottom. The 400 ml beaker was placed in a one liter glass beaker containing larval

seawater. Larval cultures were fed 40ml of the alga, *Isochrysis galbana* on the first day and 10ml of the alga, *Isochrysis galbana* plus 10ml of the alga, *Dunaliella tertiolecta* every day thereafter. Larval seawater was changed weekly and larvae were moved to beakers with 250µm nitex mesh filters when they were of adequate size (Miller and Hadfield, 1986; Gharbiah *et al*., 2008).

Development of *Ilyanassa*-specific NOS antibody

A synthetic *Ilyanassa*-specific NOS peptide was produced by Open Biosystems (Huntsville, AL). It was synthesized based on a translated 231 base-pair NOS cDNA (GenBank accession #AY763405). From the 77 amino acid sequence, a twenty amino acid portion was chosen based on its similarity to the sequence information from BIOMOL's NOS antibody that was successfully used by Thavardahara and Leise (2001) (Figure 2). The twenty amino acid peptide generated by Open Biosystems was conjugated to the carrier protein, ovalbumin. Ovalbumin was conjugated to the n-terminus in 50% of the peptides and to the c-terminus in 50% of the peptides. The ovalbumin was conjugated to the peptide to help elicit a stronger initial immune response.

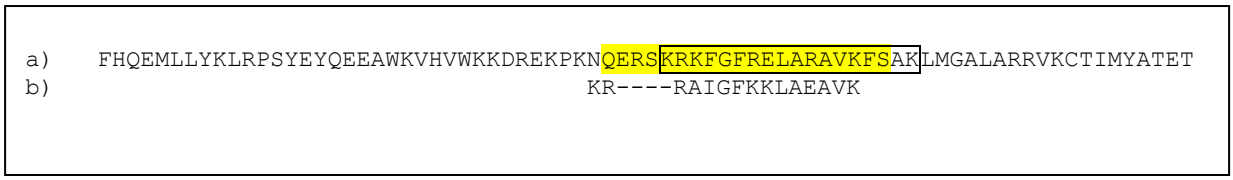

Figure 2. NOS amino acid sequence deduced from *Ilyanassa* cDNA.
a.) Deduced *Ilyanassa* NOS sequence based on cDNA (GenBank accession #AY763405). Highlighted area is the twenty amino acid sequence that was chosen for synthetic peptide synthesis. Boxed area of the sequence is the calcium-calmodulin binding domain.
b.) Sequence of the rat NOS peptide used by BIOMOL to produce neuronal NOS antibodies.

NOS antibodies were raised in two New Zealand white rabbits by Open Biosystems according to the following protocol. After the initial immunization, rabbits received booster immunizations on days 14, 28, 56 and 84. Serum was collected on days 0, 42, 70, and 98 and a terminal bleed was done on day 120. Open Biosystems did ELISA titers on day 70 and 98 serum collections. Pre-immune sera and 98 day sera was sent to me for testing on larval *Ilyanassa*, on adult tissues, and on a NOS fusion protein purified from bacteria transformed with a GST-NOS expression vector. Open Biosystems affinity-purified NOS IgGs from the rabbit that elicited a better immune response, as identified by stronger reactivity on western blots of purified bacterial produced NOS. Open Biosystems provided me with the affinity-purified antibodies as well as a sample of the peptide antigen.

Antibody testing with fusion protein

Transformation of competent bacteria

Competent DH5α bacterial cells were removed from the -80º freezer and thawed on ice, and 45µl of the thawed DH5α cells were added to 10µl of the plasmid in 999µL dH_2O. The plasmid was GEX-2T that included a DNA sequence coding for a 77 amino acid sequence of *Ilyanassa* NOS (pGEX-2T-IlyNOS(CaM)). Bacteria were left on ice for fifteen minutes with the plasmids, and then placed in a 37ºC water bath for five minutes. Five-hundred microliters of Luria-Bertani (LB) medium were added to the transformed cells and the tube was shaken at 37ºC for one hour. Various amounts of the mixture were spread on LB agar plates prepared with 50µg/ml ampicillin and grown overnight in a 37ºC incubator.

One hundred and fifty milliters of LB medium containing 50µg/ml ampicillin was inoculated with one colony from a culture plate and grown overnight in a shaker at 37ºC. The transformed bacterial culture was stored in aliquots at -80ºC.

Fusion protein induction and purification

DH5α bacterial cells transformed with pGEX-2T-IlyNOS(CaM) were grown overnight in 2ml of LB medium with 50µg/ml ampicillin at 37ºC, shaken at 200 rpm. A 1:10 dilution of the overnight culture was grown at 37ºC at 200 rpm in fresh LB medium with 50µg/ml ampicillin for four hours. Isopropyl β-D-1-thiogalactopyranoside (IPTG) to a final concentration of 0.1mM was added to the culture to induce fusion protein gene expression and the induced cells were grown at 37ºC at 200 rpm for four hours.

Microcentrifuge tubes were filled with 1.5ml of induced culture and centrifuged at 16,000 x g for one minute at room temperature. The supernatant was aspirated and the cells were frozen at -80ºC or used immediately for fusion protein purification.

Cells were resuspended in 750µl ice cold phosphate buffed saline (PBS) (137mM NaCl, 2.7mM KCl, 10.1mM Na_2HPO_4, 1.8mM KH_2PO_4, pH 7.4) containing 2µg/ml aprotinin, 2µg/ml leupeptin, 1µg/ml pepstatin A, and 2mM phenylmethylsulfonyl fluoride (PMSF). Cells were sonicated, and then Triton X-100 was added to a final concentration of 1%. The sample was centrifuged at 16,000 x g for five minutes at 4ºC and the supernatant was transferred to a fresh microcentrifuge tube. Fifty microliters of glutathione agarose (Sigma Aldrich, catalog# G4251) slurry was added to the protein sample and the sample was incubated end-over-end at 4ºC for twenty minutes.

The sample was centrifuged at 1,000 x g at 4ºC for two minutes and the supernatant was discarded. The glutathione agarose was washed with 1ml PBS with 2µg/ml aprotinin, 2µg/ml leupeptin, 1ug/ml pepstatin A and 2mM PMSF. After each wash, the sample was centrifuged at 1,000 x g at 4°C for two minutes and the supernatant was discarded. The glutathione agarose was then frozen at -80°C or prepared for electrophoresis.

Electrophoresis and western blot analysis of fusion protein

An equal volume of 2X Laemmli loading buffer with 10mM dithiothreitol (DTT) was added to the samples and the samples were heated at 100ºC for three minutes. Samples were electrophoresed on a 8 cm x 7 cm 12% acrylamide gel at 0.04 amps in

running buffer of 25mM Tris, 250mM Glycine at pH 8.3, with 0.1% sodium dodecyl sulfate (SDS).

Proteins were transferred to a nitrocellulose membrane at 100 volts for one hour on ice. The transfer took place in 25mM Tris, 250mM Glycine at pH 8.3, with 10% methanol. The nitrocellulose membrane was stained with Ponseau S to confirm protein transfer and was rinsed with distilled water. Molecular weight standards (Sigma Aldrich) were cut off of the nitrocellulose membrane and dried overnight. The remaining nitrocellulose membrane was blocked overnight in 3% non-fat dry milk in Tris-buffered saline (10mM Tris-HCl at pH 8.0, 150mM NaCl) with 0.05% Tween-20 (TBST) at 4ºC, covered, on a shaker.

The nitrocellulose membrane was incubated in primary antibody for one hour at room temperature, covered, on a shaker. The nitrocellulose membrane was either incubated in anti-glutathione-S-transferase (GST) (1:2,000), 98 day rabbit immune serum (1:1,000), rabbit pre-immune serum (1:1,000), or affinity purified anti-NOS (1:500). All primary antibodies were diluted in blocking solution. Following incubation in the primary antibody, the nitrocellulose membrane was washed in TBST with 100mM NaCl, three times for five minutes each at room temperature followed by three washes in TBST for five minutes each at room temperature.

The nitrocellulose was then incubated in alkaline phosphatase-conjugated anti-rabbit secondary antibody (Promega, catalog# S3731) at a dilution of 1:8,000 in TBST for one hour at room temperature, covered, on a shaker. Following incubation with the secondary antibody, the nitrocellulose membrane was washed in TBST with 100mM

NaCl three times for five minutes at room temperature and then washed in TBST three times for five minutes at room temperature. A final wash was done in alkaline phosphatase buffer (100mM Tris pH 9.5, 100mM NaCl, 5mM $MgCl_2$) for five minutes at room temperature. The nitrocellulose membrane was put in an alkaline phospatase buffer containing 330µg/ml nitro blue tetrazolium (NBT) and 165µg/ml 5-bromo-4-chloro-3'-indolyphosphate p-toluidine (BCIP). Once the colored reaction product was visible, the nitrocellulose membrane was taken out of the solution and dried overnight while covered with aluminum foil.

Use of NOS antibody on adult central nervous systems and larvae of *Ilyanassa*

Collection of adult central nervous systems

Adult *Ilyanassa* were placed in an anesthetic solution, 7.5% $MgCl_2$ in dH_2O, for thirty minutes. The shells of the adults were cracked with a hammer and adults were put into fresh $MgCl_2$ solution for an additional thirty minutes. Adults were removed from their shells, pinned onto a silicon dissecting dish and their central nervous systems (CNSs) were surgically removed and put on ice in FIO. Individual nervous systems were put into microcentrifuge tubes, the FIO was removed, the tubes were put on dry ice for two minutes and then frozen at -80ºC.

Collection of larvae

The size of larvae from a culture was determined by measuring 10-15 larvae under a light microscope. Larvae were collected into a small beaker with a 185µm nitex

mesh filter bottom and backwashed into a small fingerbowl with a low pH decalcifying solution (26mM $MgSO_4$, 23mM $MgCl_2$, 9mM $CaCl_2$, 9mM KCl, 423mM NaCl, 10mM Tris-HCl, pH 6) (www.mbl.edu). Larvae were decalcifed until their shells were gone (two to thirty-six hours depending on the size of the larvae). After decalcification, larvae were washed several times with FIO and put on ice until anesthetized. Aliquots of 10-100 larvae were put into microcentrifuge tubes. Anesthetized larvae were centrifuged at 1,000 x g for two minutes, after which the FIO was removed and the tubes were put on dry ice for two minutes prior to storage at -80ºC. Larvae for western blot analysis were collected at 0, 7, 11, 16-20 and 28 days post hatching (dph).

After decalcification, some competent larvae (~550µm in size and 16-20dph) were cultured in 10 mM serotonin in FIO for two to twenty four hours. The larvae were then washed with FIO several times and processed for storage at -80^{o}C as described above.

Solubilization and electrophoresis of adult central nervous system and larval proteins

Adult central nervous systems were homogenized by adding 50µl of solubilization buffer (SB) (100mM NaCl, 50mM Tris-HCl pH 7.5, 1% IGEPAL (Sigma Aldrich, catalog# I3021), 2mM PMSF, 1µg/ml aprotinin, 1µg/ml leupeptin and 1µg/ml pepstatin A) per adult central nervous system and pipetted for about twenty seconds. Total larval proteins were obtained from fifty to five hundred larvae by homogenization in 50-1,000 µl of SB. For samples prepared from both adult CNSs and total larval proteins, samples were placed on ice for three minutes and then homogenized using a

Dounce homogenizer. The homogenate was put back into the microcentrifuge tube and spun at 4,000 x g at 4ºC for two minutes. The supernatant was put into a new microcentrifuge tube and an equal volume of 2X Laemmli buffer with DTT was added. The sample was heated at 100ºC for three minutes and electrophoresed on a 6% acrylamide gel at 0.04 amps.

TCA precipitation and electrophoresis of adult central nervous system and larval proteins

Frozen larvae and adult CNSs were homogenized in SB as described above. After putting the homogenate into a new tube, total protein of each sample of larval extract was determined by BCA protein analysis (Thermo Scientific, Catalog #23227) and sample volumes were adjusted with SB for equal concentrations of total larval proteins in each sample. To each sample 10% trichloroacetic acid (TCA) was added to precipitate total larval proteins and the samples were incubated on ice for thirty minutes. The samples were centrifuged at 16,000 x g for fifteen minutes at 4°C. The supernatant was removed and the inner walls of the microcentrifuge tube were dried with a Kimwipe to remove excess moisture and unpelleted material. The pellet was washed twice with 300µl of cold acetone and centrifuged at 16,000 x g for five minutes at 4°C. The supernatant was removed and the pellet was allowed to air dry for thirty minutes. The pellet was resuspended in 2X Laemmli loading buffer by sonication and use of a Dounce homogenizer. The samples were electrophoresed on a 16 cm x 16 cm 7% acrylamide gel at 0.08 amps to maximize sample size and protein separation. The portion of the

acrylamide gel containing proteins in the 130-160kd range was cut to the size of a mini-gel (8cm x 7 cm) for transfer to nitrocellulose for western blot analysis. Protein transfer and western blot analysis were done as described above.

Western blot analysis of adult central nervous systems and larval proteins

Proteins were transferred to nitrocellulose as described above. The nitrocellulose was either incubated in rabbit pre-immune serum, affinity purified anti-NOS IgGs or affinity-purified anti-NOS IgGs pre-absorbed with the target peptide. The affinity purified anti-NOS antibody (1:500) and the peptide (1:125) were incubated in blocking solution for one hour before being added to the nitrocellulose. Western blot analysis was done as described above.

Determining optical densities of proteins

For western blots of developing and metamorphosing larvae, the optical density of each band was determined using ImageJ (version 1.42) using a scanned image. ImageJ is a program that gives a numerical value for pixel intensity in a defined area. Boxes were drawn around bands of interest. The optical density (pixel intensity value) of the band was divided by the lowest optical density of all bands examined to determine the fold increase. Graphs were produced in Microsoft Office Excel 2003.

Probe preparation

Linearization and purification of plasmids for probe synthesis

Plasmids containing *Ilyanassa* NOS and actin inserts were linearized by restriction endonuclease digestion and purified for use as templates in probe synthesis. pBS-IlyNOS(CaM), the Bluescript plasmid containing a 231 base-pair *Ilyanassa* NOS insert (Fowler, 2005) was digested with EcoRI or BamHI for sense and anti-sense probe synthesis, respectively. pBS-IlyAct, the Bluescript plasmid containing a 297 base-pair *Ilyanassa* actin insert (Fowler, 2005), was also digested with BamHI and EcoRI for sense and anti-sense probe synthesis, respectively. Endonuclease digestions were carried out for two hours at 37°C. To confirm that the plasmid was cut, 1µl of the reaction mixture diluted in 9µl of loading buffer was electrophoresed at 100 volts on a 1% agarose gel in 40mM Tris-acetate, 1mM EDTA (TAE) with 1µg/ml ethidium bromide added. DNA was visualized by UV light.

Digested DNA was purified as follows: An equal volume of phenol/chloroform was added to the reaction mixture, vortexed and centrifuged at 16,000 x g for three minutes. The supernatant was put into a new tube and an equal volume of chloroform was added. The sample was then vortexed and centrifuged at 16,000 x g for three minutes. The supernatant was put into a new tube and a volume equal to 0.1 times the volume of supernatant of 3M Sodium Acetate and a volume equal to 2.5 times the volume of supernatant of 100% ethanol was added. The sample was vortexed and centrifuged at 16,000 x g for fifteen minutes at 4°C. The supernatant was removed and the pellet was resuspended in 500µl of 70% ethanol. The sample was centrifuged at

16,000 x g for ten minutes at 4°C. The supernatant was removed and the pellet was dried using a speed-vac and resuspended in 10µl of diethylpyrocarbonate (DEPC)-treated water. The presence of the purified linearized plasmid was verified by gel electrophoresis as stated above and quantified using a nanodrop spectrophotometer. All linearized plasmids were diluted to approximately 1µg/µl and stored at -20°C.

Probe synthesis

NOS sense and anti-sense and actin sense and anti-sense mRNA probes were synthesized from the linearized plasmids. Ribonucleoside triphosphates (rNTPs) were prepared on ice for the probe synthesis. rNTPs consisted of 2.5mM rATP, 2.5mM rGTP, 2.5mM rCTP, 1.6mM rUTP and 0.9mM digoxygenin-labeled rUTP (Roche Applied Science, catalog# 11209256910). 1-2µg purified plasmid was added to 1X transcription buffer, 10mM DTT, 10µl rNTPs and DEPC treated water and 0.2U/µl RNasin (Promega, catalog# N2111) and 1.2U/µl of the appropriate polymerase were then added. T3 RNA polymerase (Promega, catalog# P2083) was added to pBluescript with both NOS and actin inserts cut with EcoRI. T7 RNA polymerase (Promega, catalog# P2075) was added to pBluescript with both NOS and actin inserts cut with BamHI. All components were combined at room temperature. The reaction mixture was incubated for two hours at 37°C. After two hours, 1µl of the reaction mixture was run on a 1% agarose in TAE gel with 1µg/ml ethidium bromide added to confirm RNA synthesis.

DNase I was added to each reaction sample to a final concentration of 0.02 µg/ml and incubated at 37°C for ten minutes. Each sample was purified through a G-50 spin

column (Amersham Bioscience, catalog# 27533001) and 1µL of each reaction was removed for Northwestern blot analysis. One tenth volume of 3M sodium acetate and 2.5 volume of 100% ethanol was added to the remaining sample. The samples were vortexed, put on dry ice for five minutes and centrifuged for fifteen minutes at 16,000 x g at 4°C. The supernatant was removed and the pellet was resuspended in 500µl of 70% ethanol. The supernatant was removed and the pellet was dried in a speed-vac. The pellet was resupended in 1.5ml hybridization buffer (50% formamide, 5X RNase free sodium chloride sodium citrate buffer (SSC) (20X SSC- 3M NaCl, 0.3M Sodium citrate, pH 7.0) with 1mg/ml Torula RNA, 1X Heparin, 1X Denhart's, 0.1% Tween-20, 0.1% CHAPS, 5mM RNase free EDTA) and then stored at -20°C.

Northwestern blot to confirm digoxygenin-labeled uracil incorporation in probes

One µL of each probe was lyophilized with a speed-vac and then 2-4µl of 10X RNase free HEPES/EDTA in DEPC-treated water was added to each sample and 4-6µl of 250µl formamide mixed with 89µl formaldehyde was added to the sides of each tube and centrifuged to the bottom of the tube. The samples were heated at 70°C for ten minutes and then quenched on ice for five minutes. Condensation in the tube was returned to the bottom of the tube by momentary centrifugation and 1.5µl RNA loading buffer was added. The samples were electrophoresed on a 6% agarose gel containing 1X HEPES/EDTA and 6% formaldehyde and electrophoresed at 90-95 volts for one hour. After electrophoresis, the gel was rinsed with water and equilibrated in 20X SSC for one hour. The gel was transferred overnight to nitrocellulose by capillary action in 20X SSC.

The RNA was cross-linked to the membrane using a Stratalinker (Stratagene, Inc.). Cross-linking uses UV light to covalently link amine groups of RNA to the membrane. The membrane was washed in 100mM Tris pH 7.5, 150mM NaCl (buffer 1) for five minutes and then blocked with 0.5% blocking reagent (Boehringer Mannheim, catalog# 109176) in 100mM Tris pH 7.5, 150mM NaCl (buffer 2) for thirty minutes at room temperature. The membrane was incubated with an anti-digoxygenin polyclonal antibody diluted 1:5,000 (Roche Applied Science, catalog# 11093274910) in buffer 1 for thirty minutes at room temperature and then washed twice for fifteen minutes with buffer 1. The membrane was then equilibrated in 100mM Tris pH 9.5, 100mM NaCl, 50mM $MgCl_2$ (buffer 3) by washing twice for five minutes. RNA probes were visualized by incubating the membrane in buffer 3 containing 0.17µg/uL NBT and 0.09µg/uL BCIP.

In situ hybridization of larval *Ilyanassa*

Collection of larvae for in situ *hybridization*

Competent larvae were sized and decalcified as stated earlier. After decalcification, larvae were washed several times with FIO and put into vials on ice until anethetized and FIO was removed. A fixation solution containing 0.1M 3-[N-morphlino] propanesulfonic acid (MOPS), pH 7.2, 2mM EGTA, 1mM magnesium sulfate and 3.7% formaldehyde (MEMFA) was added. The larval specimens were incubated in fixative for two hours at room temperature on a rocker. After the incubation, a solution of 50% methanol and 50% FIO was added for twenty minutes followed by 100% methanol twice for ten minutes. The vials of larvae were stored in 100% methanol at -20°C.

In situ *hybridization*

Fixed larval specimens were rehydrated in methanol and PBS with 0.1% Tween-20 (PTW). Rehydration was conducted by subjecting specimens to five minute washes at room temperature in 75% methanol/25%PTW, 50% methanol/50%PTW, and 25% methanol/75%PTW. Finally, specimens were washed for five minutes at room temperature in 100% PTW four times. Specimens were incubated in 5ml PTW containing 5µg/µL proteinase K (Boehringer Mannheim) for twenty-five minutes. Specimens were washed twice for five minutes each in 5ml 100mM triethanelamine (TEA) pH 7-8 after which 12.5µl of acetic anhydride was added to the vial and after five minutes an additional 12.5µl of acetic anhydride was added. After five more minutes, the specimens were washed twice for five minutes in 5ml PTW and refixed in 4% paraformaldehyde in PTW for twenty minutes at room temperature. Refixation was followed by five washes in 5ml PTW. All but 1ml of the final PTW was removed and 250µl of hybridization buffer was added to each vial. Specimens were allowed to settle to the bottom of the vial before the mixture was removed and replaced with 500µl hybridization buffer. The vials were incubated for two hours at 60°C. The hybridization buffer was replaced with 500µl fresh hybridization buffer and incubated for six hours to overnight at 60°C. After the incubation, the hybridization buffer was replaced with 1µg/ml of the appropriate RNA probe in hybridization buffer and the specimens were incubated overnight at 60°C.

The following day, specimens were washed with 5ml fresh hybridization buffer for ten minutes at 60°C and then with 2X SSC three times at 65-70°C for twenty minutes

each wash. Specimens were then incubated in 20µg/ml RNase A (Promega) and 10U/ml RNase T (Boehringer Mannheim) in 2X SSC for thirty minutes at 37°C. Specimens were washed in 2X SSC for ten minutes at room temperature and for thirty minutes at 60°C in 0.2X SSC. This wash was followed by three 10 minute washes in malonic acid buffer (100mM Malonic acid, 150mM NaCl; MAB) at room temperature. Specimens were then blocked for one hour in MAB containing 20% heat-inactivated lamb serum. The blocking solution was replaced with MAB, 20% heat-inactivated lamb serum and a 1:2,000 dilution of anti-digoxygenin polyclonal antibody and incubated at room temperature for four hours. After incubation with the antibody, the specimens were rinsed twice with MAB and washed twice for two to four hours at room temperature with MAB before a final overnight wash at 4°C in MAB.

After the overnight wash with MAB, specimens were washed in fresh MAB for thirty minutes before being washed twice with alkaline phospatase buffer (100mM Tris pH 9.5, 50mM $MgCl_2$, 100mM NaCl, 0.1% Tween-20, 5mM levamisole) for five minutes each, at room temperature. RNA probe-mRNA hybrids were visualized by incubating the specimens in alkaline phospatase buffer containing 4.5µL/mL NBT and 3.5µL/mL BCIP for approximately two hours. To stop the color reaction, PBS containing 4% paraformaldehyde was added. The specimens were washed in 100% methanol for one hour and stored in fresh methanol at 4°C. Specimens were either viewed with an Olympus BX-60 bright field microscope as whole mounts or sectioned in paraffin and mounted on subbed slides (see below). Slides were viewed on an Olympus BX-60

compound microscope under bright field illumination. Images were captured with a Nikon N90S digital camera and processed with Adobe Photoshop version 8.0.

Paraffin sectioning of larval specimens from in situ *hybridization*

Specimens were transferred to fresh 100% ethanol and then washed twice for five minutes each in 100% ethanol. Half of the ethanol was replaced with Hemo-De (Fisher Scientific, catalog# 15182507A), a solvent and clearing agent, and held at room temperature for five minutes. Half of the Hemo-De/ethanol mixture was replaced with fresh Hemo-De and held at room temperature for ten minutes. This step was repeated once after which all of the Hemo-De/ethanol mixture was replaced with fresh Hemo-De and held at room temperature for ten minutes. The Hemo-De was replaced with fresh Hemo-De and held for fifteen minutes at room temperature and then half of the Hemo-De was replaced with molten paraffin and held at 55°C for ten minutes. The Hemo-De/paraffin mixture was replaced with molten paraffin and held at 55°C for ten minutes. This step was repeated twice except the vials were held at 55°C for thirty minutes and then overnight. Individual larval specimens were embedded in paraffin molds and 10-12µm sections were obtained using a Microm HM315 rotary microtome. Sections were attached to slides prepared with a subbing solution (Presnell and Schreiban, 1997). No counterstain was used. Slides were viewed and images were captured and processed and as stated above.

CHAPTER III

RESULTS

I wanted to determine the location and temporal expression pattern of neuronal NOS (nNOS) during larval development. Because none of the commercially available antibodies would recognize *Ilyanassa* NOS, I developed a species-specific polyclonal antibody directed specifically to *Ilyanassa* nNOS. A synthetic peptide based on the deduced amino acid sequence of an *Ilyanassa* cDNA (Figure 3b) was used to immunize two New Zealand White rabbits (see Materials and Methods). Immunogenic response was monitored for several months. *Ilyanassa*-NOS sequence specific IgGs were purified and used to investigate larval expression of NOS protein. Sera collected from rabbits immunized with NOS peptides were assayed by ELISA for NOS reactivity. The titre of NOS-specific reactivity was also tested by western blotting of bacterially produced GST-*Ilyanassa* NOS fusion protein (Figure 3c). After the specificity of the polyclonal antibody was verified, the antibodies were used to investigate temporal and spatial expression of nitric oxide synthase in larval *Ilyanassa*.

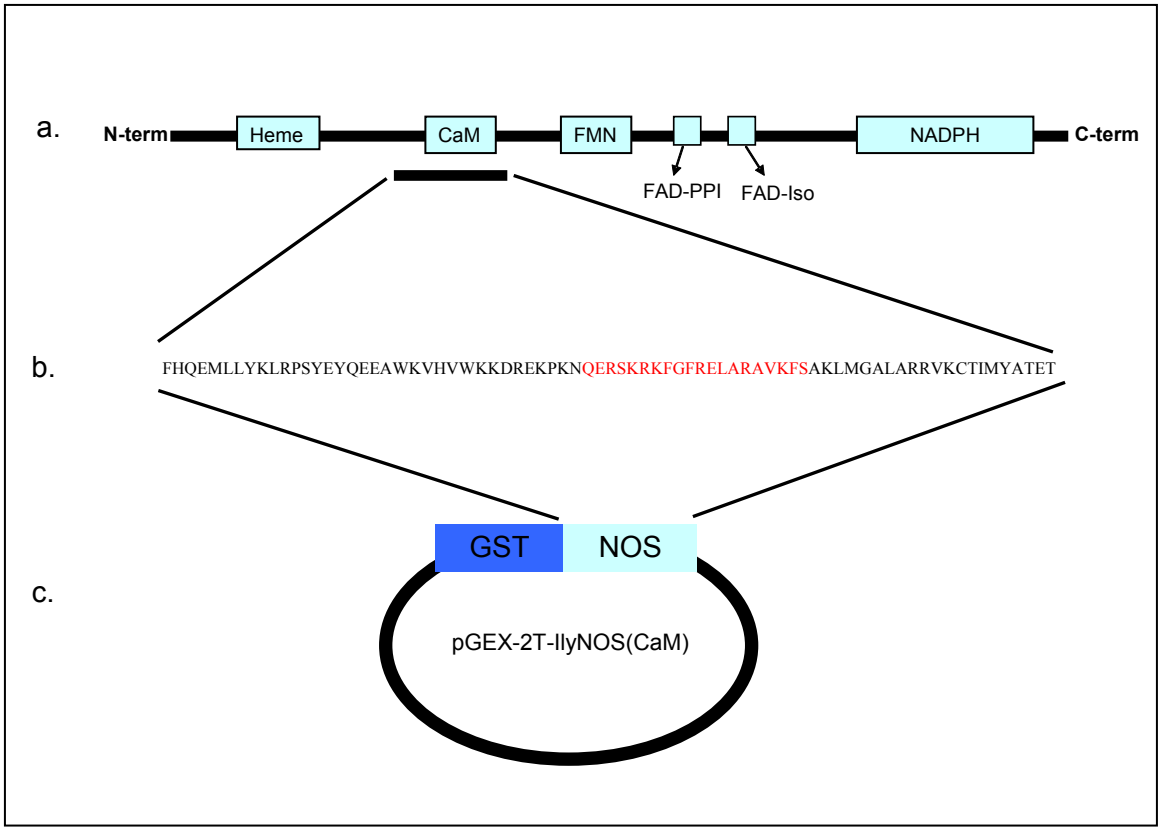

Figure 3. Schematic diagram of NOS protein and pGEX-2T-IlyNOS(CaM). An *Ilyanassa*-specific peptide (b in red) was used to immunize New Zealand White rabbits. Sera was collected from the rabbits and tested for immunogenic responses to bacterial produced *Ilyanassa*-specific NOS protein fused to GST (c). The peptides used for both the immunizations and fusion protein are part of the calcium-calmodulin binding domain (CaM) in (a).

Testing of NOS-specific antisera

During the immunization period, NOS peptide reactivity of the rabbit sera was monitored at Open Biosystems by an enzyme-linked immune assay (ELISA). Forty-two days after the initial injection, rabbit D4084 had an ELISA titer of 400 and D4085 had a titer of 100 (These values represent the reciprocal of the serum dilution point where the absorbance drops below 0.2 at OD_{405}.) Pre-immunization titers from the sera of both rabbits were less than 50. Ninety-eight days after the first inoculation of the rabbits, rabbits D4084 had an ELISA titer of 400 and D4085 had a titer of 200.

Crude D4084 and D4085 sera were tested by western blotting to determine which of the sera had greater NOS epitope reactivity and therefore would be used for NOS-specific IgG purification. GST-NOS fusion protein was electrophoresed, transferred to nitrocellulose, and probed with the crude 98 day sera (Figure 4). Antibodies in both sera recognized a polypeptide of M_r 35 kDa representing the GST-NOS fusion protein (Figure 4b; lanes 6 and 10), but failed to recognize the 29 kDa GST in the adjacent lane (Figure 4b; lanes 5 and 9). In comparison, an anti-GST antibody recognized bands of 33 kDa and 28 kDa in the GST-NOS lane (Figure 4b; lane 2) and a band of 26 kDa in the GST lane (Figure 4; lane 1). Pre-immune sera from both rabbits and secondary antibody in the absence of a primary antibody failed to recognize any bands in replicate blots. These results indicated that antibodies from both rabbits recognized the GST-NOS fusion protein to similar degrees. However, since the serum from rabbit D4084 had a stronger response as measured by ELISA, this serum was selected for affinity purification of antibodies for further use in the study.

a

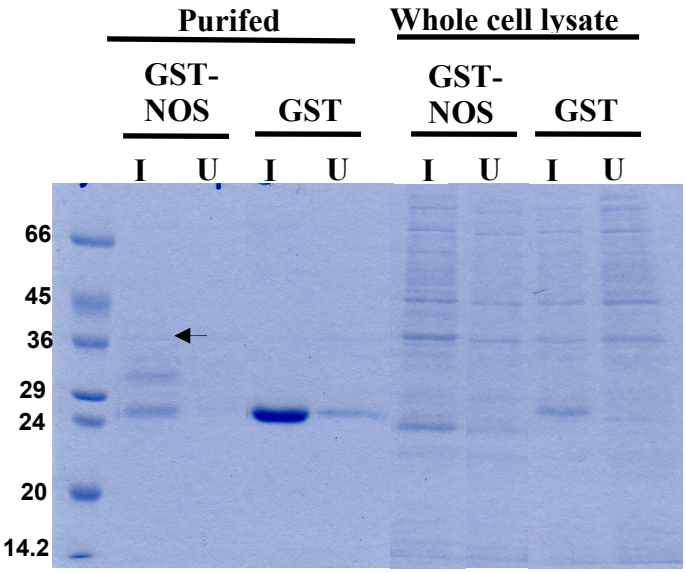
Purifed
Whole cell lysate
GST-NOS
GST
GST-NOS
GST
I U I U I U I U
66
45
36
29
24
20
14.2

b

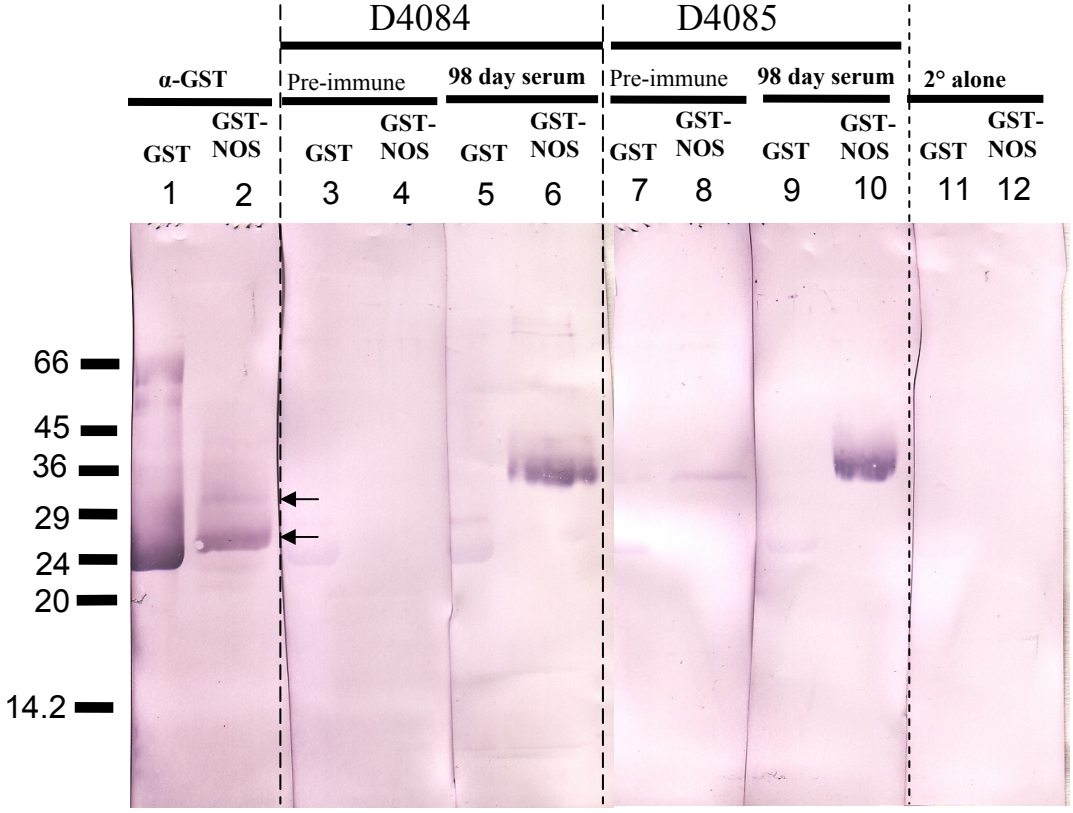
D4084
D4085
α-GST
Pre-immune
98 day serum
Pre-immune
98 day serum
2° alone
GST GST-NOS GST GST-NOS GST GST-NOS GST GST-NOS GST GST-NOS GST GST-NOS
1 2 3 4 5 6 7 8 9 10 11 12
66
45
36
29
24
20
14.2

Figure 4. Analysis of crude 98-day anti-NOS sera by western blot. GST and GST-NOS fusion protein were purified from IPTG-induced (I) and uninduced (UI)-DH5α bacterial cells transformed with GST-NOS or GST alone and electrophoresed on 12% polyacrylamide gels. (a) Coomassie Brilliant Blue gel (b) Western blot of companion gel probed with pre-immune serum from each rabbit, D4084 and D4085, (lanes 3, 4, 7 and 8), anti-NOS serum from each rabbit (lanes 5, 6, 9 and 10), anti-GST (lanes 1 and 2), or anti-rabbit alkaline phosphatase-conjugated secondary antibody alone (lanes 11 and 12). Induction causes synthesis of proteins as expected. Bands indicated by arrows are the presumptive NOS proteins. In "a", arrow indicates the presumptive 38kDa full length GST-NOS. In "b" top arrow indicates 33 kDa polypeptide and bottom arrow indicates 28 kDa polypeptide. Molecular weight markers are indicated in kilodaltons.

Testing of affinity purified NOS antibody on fusion protein

Ilyanassa NOS-specific antibodies were purified from the 98-day D4084 serum by affinity chromatography using the NOS peptide immunogen conjugated to cross-linked Sepharose beads. To confirm that the affinity purified NOS immunoglobulins had retained their ability to recognize the NOS epitope through the purification process, western blot analysis was performed on purified GST-NOS fusion protein (Figure 5). Affinity purified IgG from the D4084 serum (D4084-AP) recognized at least three polypeptides in the GST-NOS sample, including a major band of M_r 34 kDa and two minor bands M_r 36 kDa and 39 kDa (Figure 5; lane 2). Anti-GST recognized similar polypeptides in this sample, as well as a dense band of approximately 30 kDa (Figure 5; lane 4). The anti-GST antibody recognized a major polypeptide of M_r 29 kDa in the purified GST sample (Figure 5; lane 3) and several higher molecular weight polypeptides, likely representing multimers of GST. The D4084-AP antibody failed to recognize anything in that sample (Figure 5; lane 1).

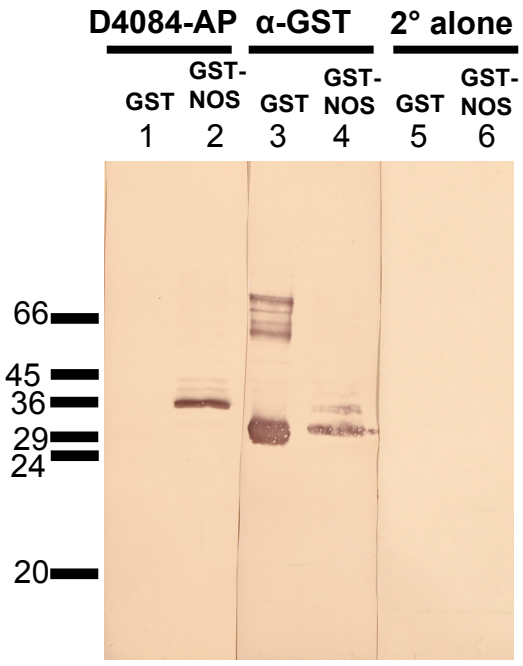

Figure 5. Western blot recognition of GST-NOS fusion protein by affinity-purified anti-NOS antibody, D4084-AP. GST (lanes 1, 3, and 5) and GST-NOS (lane 2, 4, and 6) fusion protein were purified from bacterial lysates, electrophoresed on a 12% polyacrylamide gel, transferred to nitrocellulose and probed with D4084-AP, anti-GST or alkaline phosphatase-congugated anti-rabbit secondary antibody alone. D4084-AP recognized a major polypeptide of M_r 34 kDa in the GST-NOS sample (lane 2). Anti-GST antibodies recognized a polypeptide of similar size in addition to another more prominent band of M_r 30 kDa (lane 4). The anti-GST antibody reacts strongly with purified GST (lane 3), whereas D4084-AP does not (lane 1). Molecular weight markers are indicated in kilodaltons.

Testing of affinity purified NOS antibody on larval extracts

Once it was determined that the affinity purified NOS antibody recognized the *Ilyanassa* NOS epitope, detergent extracts of larval *Ilyanassa* were western blotted and probed with D4084-AP to see if the affinity-purified antibody could detect endogenous NOS in larval *Ilyanassa*. Since the actual amount of NOS in larvae is expected to be relatively small, extracts from 10 to 100 competent larvae were prepared to optimize the conditions needed to test the anti-NOS antibody. Competent larvae were used because they were expected to have the highest concentration of neuronal NOS.

The larvae were homogenized in SB, electrophoresed on a 6% polyacrylamide gel, transferred to nitrocellulose, and probed with D4084-AP antibody (Figure 6). Broad, poorly defined bands of M_r 183 kDa, 116 kDa, 89 kDa and 66 kDa were recognized by the D4084-AP antibody. These bands are most easily seen in the lanes with the extract prepared from 100 larvae.

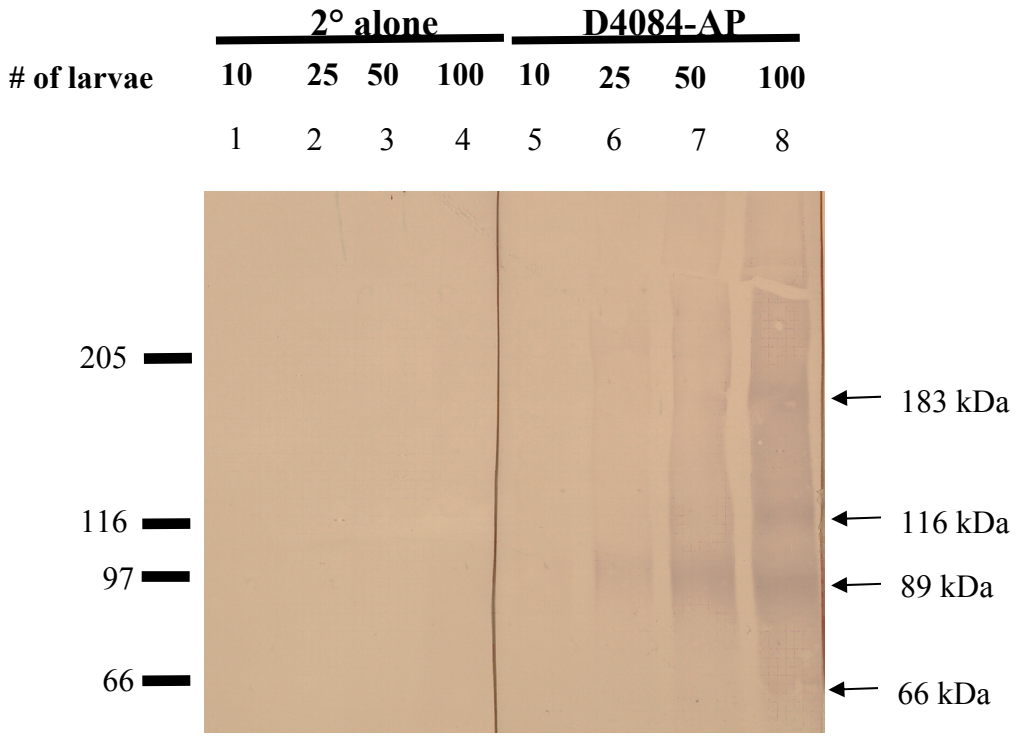

Figure 6. Western blot analysis of D4084-AP immunoreactivity to NOS in larval *Ilyanassa*. Samples of 10, 25, 50 or 100 larvae were homogenized in SB, electrophoresed on a 6% polyacrylamide gel, transferred to nitrocellulose and probed with the D4084-AP antibody or alkaline phosphatase-conjugated anti-rabbit secondary antibody alone. Broad bands of approximately 183 kDa, 116 kDa, 89 kDa and 66 kDa were recognized by the D4084-AP antibody. Molecular weight markers are indicated in kilodaltons.

Testing of affinity purified NOS antibody on adult brains

Since the western blots of the larval extracts did not convincingly demonstrate D4084-AP recognition of *Ilyanassa* NOS, an alternative source of *Ilyanassa* NOS was obtained. Brains of adult *Ilyanassa* were dissected, homogenized and extracted in SB. The extracts were electrophoresed, transferred to nitrocellulose and probed with the affinity purified D4084-AP antibody (Figure 7). Five polypeptides of M_r 176 kDa, 157 kDa, 102 kDa, 88 kDa and 66 kDa were recognized by the antibody (Figure 7; lane 3). To verify the specificity of recognition, the D4084-AP antibody was preabsorbed with the NOS peptide immunogen prior to incubation with the blot. The 102 kDa and 88 kDa bands were recognized by the pre-absorbed antibodies as well as by antibodies in the pre-immune serum (Figure 7; lane 4 and 2, respectively). However, the polypeptides of M_r 176 kDa, 157 kDa, and 66 kDa were no longer recognized by the preabsorbed D4084-AP (Figure 7; lane 4).

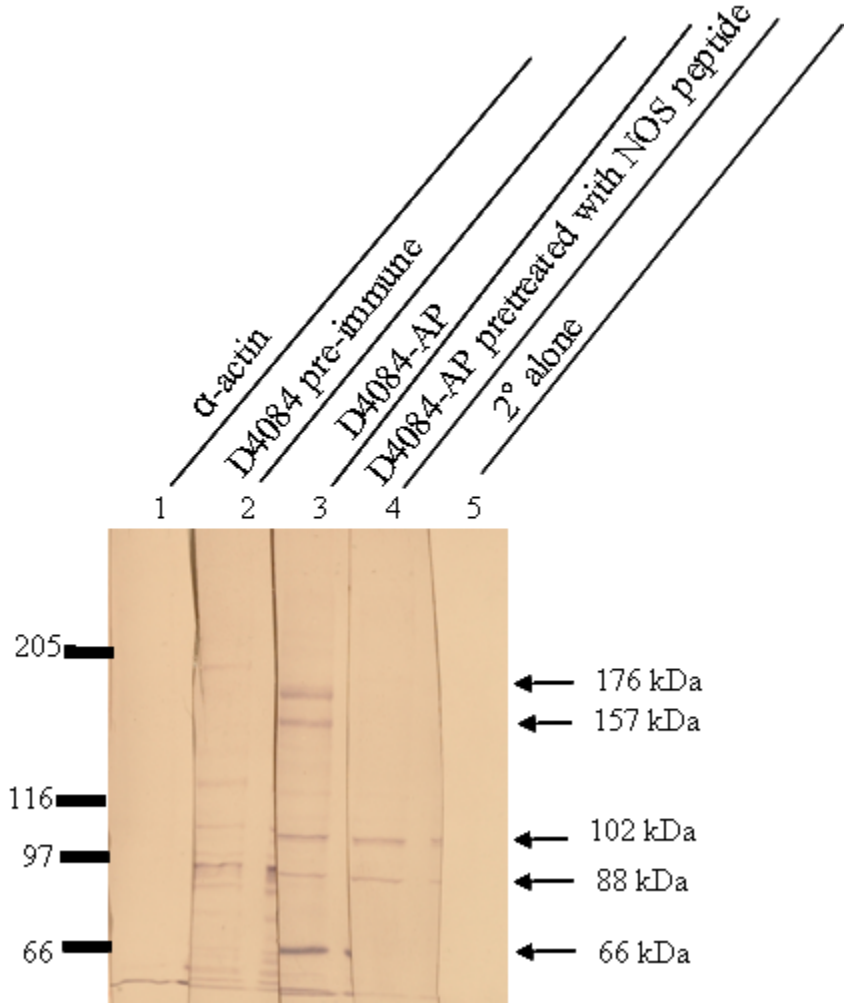

Figure 7. Western blot analysis of D4084-AP immunoreactivity to NOS in brains of adult *Ilyanassa*. Isolated brains were homogenized in SB, electrophoresed on a 6% polyacrylamide gel, transferred to nitrocellulose, and probed with D4084-AP (lane 3), D4084-AP pre-treated with NOS peptide (lane 4), or D4084 pre-immune serum (lane 2). Recognition by D4084-AP of polypeptides of M_r 176 kDa, 157 kDa and 66 kDa was eliminated by preabsorption of the antibody with the *Ilyanassa* NOS peptide antigen (lane 4). Identical samples were probed with an anti-actin antibody (lane 1) and with alkaline phosphatase-conjugated anti-rabbit secondary antibody alone (lane 5) as controls. Molecular weight markers are indicated in kilodaltons.

Temporal expression of NOS in larval *Iyanassa*

Since D4084-AP specifically recognized presumptive NOS epitopes in nervous tissue from adult *Ilyanassa,* the antibody was used to investigate potential changes in the amount of NOS present during larval development. In western blots of larval extracts, D4084-AP recognized relatively high amounts of polypeptides of M_r 116 kDa and 89 kDa (Figure 6). Two less prominent bands, M_r 183 kDa and 66 kDa (Figure 6) were also visible. To enrich the 183 kDa and 66 kDa polypeptides in the samples for western blotting, total protein from 1000-500 larvae at different developmental stages was concentrated by precipitation with TCA (protein concentration was adjusted before TCA precipitation for equal total protein concentration in each sample). The precipitated larval proteins were analyzed by western blot using the D4084-AP antibody (Figure 8). A band at M_r 66 kDa (Figure 6) was recognized by the antibody in proteins from 0, 7, 11, and 18 DPH larvae. A single polypeptide of 60 kDa was recognized in 28 DPH larval proteins.

To detect changes in nNOS polypeptides during metamorphosis, physiologically competent larvae were induced with 5-HT. Larvae were collected at zero, two, six, eighteen and twenty-four hours after induction. Total protein from 500 metamorphosing larvae (adjusted for equal total protein concentration) was precipitated with TCA and analyzed by western blot, again using the D4084-AP antibody (Figure 9).

Because the D4084-AP antibody recognized putative NOS epitopes, we used this antibody to test the hypothesis that NOS levels decrease following onset of metamorphosis. To determine if the levels of nitric oxide synthase were increasing or

decreasing during larval development and metamorphosis, the optical density of each band was determined using ImageJ. Figures 10 and 11 graphically show the fold change in optical density of the 66 kDa NOS polypeptide. Optical densities of the 66/60 kDa polypeptide fluctuated in the western blot of developing larvae (Figure 10). NOS optical densities at zero dph were twice as dense as at seven dph. The optical density at 11 dph was the lowest but only slightly lower than seven dph. At competency (18 dph), NOS levels once again elevated. Larvae that were 28 dph had an optical density close to that of 11 dph larvae.

For NOS levels of metamorphosing larvae, optical density decreased over time following induction of metamorphosis by 5-HT (Figure 11). Competent larvae (zero hours) had three fold higher levels of NOS compare to the lowest level at 18 hours of induction. From zero hours to 18 hours after induction, optical densities steadily decreased. At 24 hours after induction, the optical density was similar to that of the zero hour time point. The non-induced 24 hour control had an optical density much higher than even the zero or 24 hour induction.

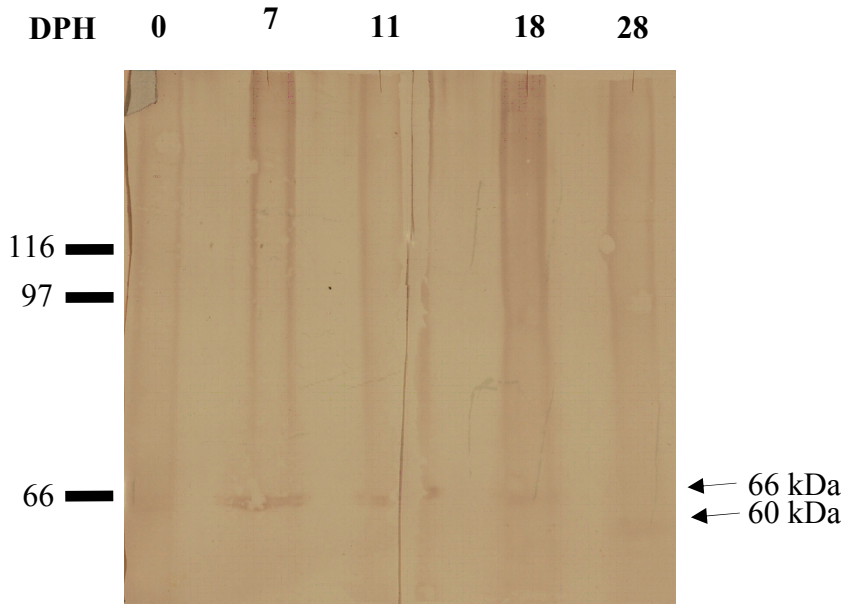

Figure 8. Western blot analysis of neuronal NOS levels during larval development. 1000-500 Larvae were collected at 0, 7, 11, 18 and 28 days post-hatching (DPH) and homogenized in SB. Equal amounts of total larval proteins were precipitated from the extracts using TCA, electrophoresed on an 8% polyacrylamide gel, transferred to nitrocellulose , and probed with D4084-AP. A single band of 66 kDa is recognized in extracts of 0, 7, 11 and 18 DPH larvae and 60 kDa band was detected in 28 DPH (indicated by the arrows). Molecular weight markers are indicated in kilodaltons.

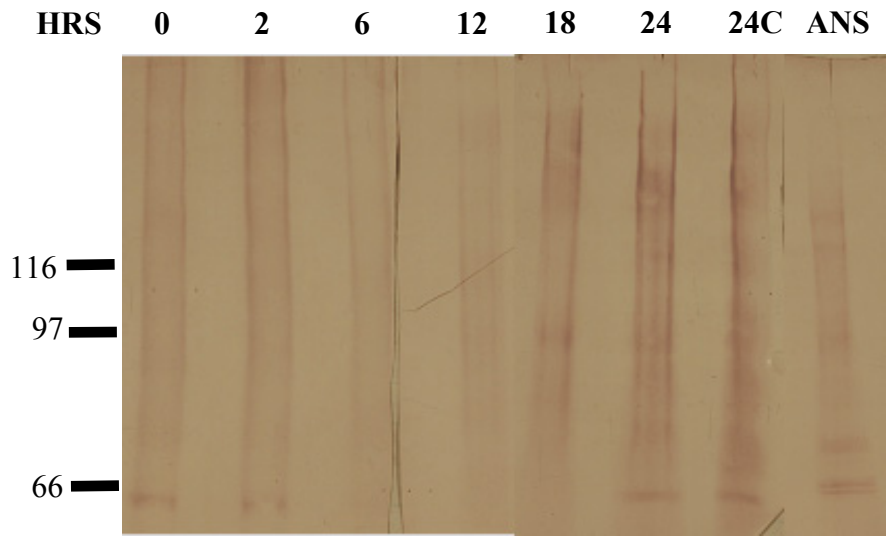

Figure 9. Western blot analysis of neuronal NOS levels during larval metamorphosis. Competent larvae were induced to metamorphose with serotonin, collected at 0, 2, 6, 12, 18, and 24 hours after induction, then 500 larvae at each time point were homogenized in SB. Equal amounts of total larval proteins were precipitated from the extracts using TCA, electrophosesed on an 8% polyacrylamide gel, transferred to nitrocellulose, and probed with the D4084-AP antibody. Homogenized adult central nervous systems (ANS) and TCA-precipitated proteins from uninduced larvae collected after 24 hours in FIO were used as controls. The arrow indicates the 66 kDa band that was detected in all of the samples. Molecular weight markers are indicated in kilodaltons.

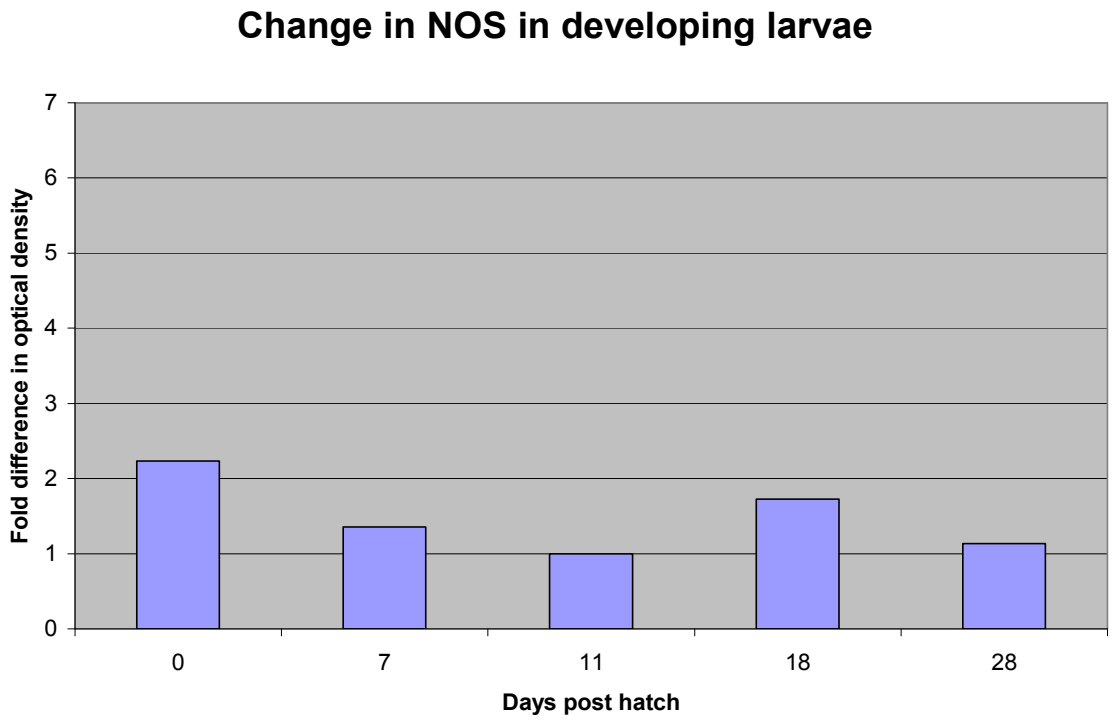

Figure 10. Optical density (OD) measurements of the 66kDa band from the western blot in Figure 8. Analysis of changes in NOS levels during larval development were determined for each time point and plotted in relation to the fold change in optical density. The levels of NOS fluctuated during larval development as indicated by the optical densities.

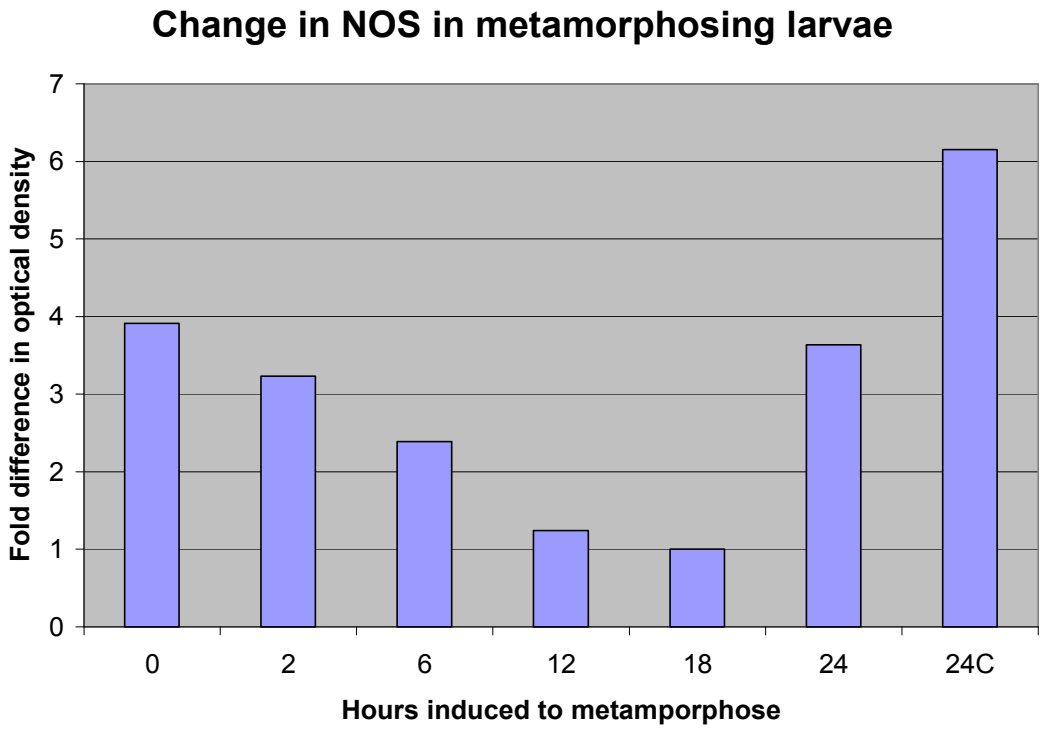

Figure 11. Optical density (OD) measurements of the 66kDa band from the western blot in Figure 9. Analysis of changes in NOS levels following 5-HT induction of metamorphosis. Levels of NOS decreased during metamorphosis but increased to pre-metamorphosis levels 24 hours after induction of metamorphosis.

Localization of NOS transcripts in larval *Ilyanassa*

The relationship between gene expression and the presence of a protein can be complex and may not follow predictable spatial or temporal patterns of occurrence during development. To determine the location of gene expression in larval *Ilyanassa*, *in situ* hybridization was conducted on fixed competent larvae.

NOS and actin probes were synthased from *Ilyanassa*-specific cDNAs. After linearization and purification of the cDNAs, RNA was synthesized to contain digoxygenin-labeled rUTP. A northwestern blot were performed to confirm the correct size of the probe and labelled uracil incorporation into the probe (Figure 12). The Northwestern blot confirmed digoxygenin-labelled probes by use of an anti-digoxygenin antibody and confirmed the correct sizes of probes with 231 bases for NOS probes and 297 bases for the actin probes.

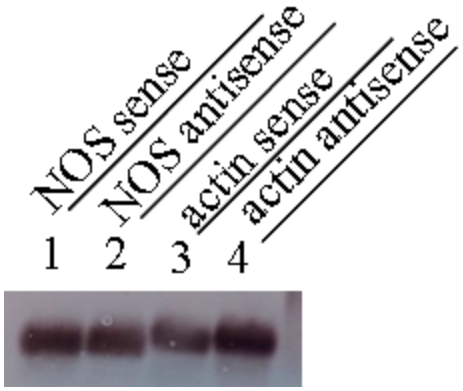

Figure 12. Northwestern blot analysis of NOS and actin RNA probes. Incubation of the cross-linked RNA probes with anti-digoxygenin antibody indicted NOS probes of 231 bases and actin probes of 297 bases.

Competent larvae were then treated as described with anti-sense NOS and actin probes and sense NOS and actin probes and examined as whole mounts by bright field microscopy. Sense probes served as negative controls and the anti-sense actin probe served as a positive control. Larvae treated with the actin anti-sense probe showed staining in all areas of the larva (Figure 12b). Treatment of competent larvae with NOS anti-sense probes displayed hybridization in areas of the posterior region of visceral mass (Figure 13a, white arrow), possible staining near the mouth (Figure 13b, white arrowhead) and non-specific staining on the edge of the velar lobe (Figure 13a, VL). Larvae treated with sense NOS and sense actin probes showed some non-specific staining on the edges of the visceral mass (Figure 13c and d).

To determine more precisely the cellular location of the NOS anti-sense hybridization and to determine if NOS mRNAs were expressed in cells of any larval ganglia, larvae were embedded in paraffin and sectioned (Figure 14). Examination of 10 micrometer sections treated with the anti-sense NOS probe revealed localization of NOS mRNA in the visceral mass of the larva (Figure 14b, white arrow) but no evidence of staining in the head in the general location of the AG (Figure 14a). No evidence of anti-sense probe was observed in the head region or in any ganglia of the central nervous system. Larvae treated with the anti-sense actin probe displayed general overall actin gene expression (Figure 14c).

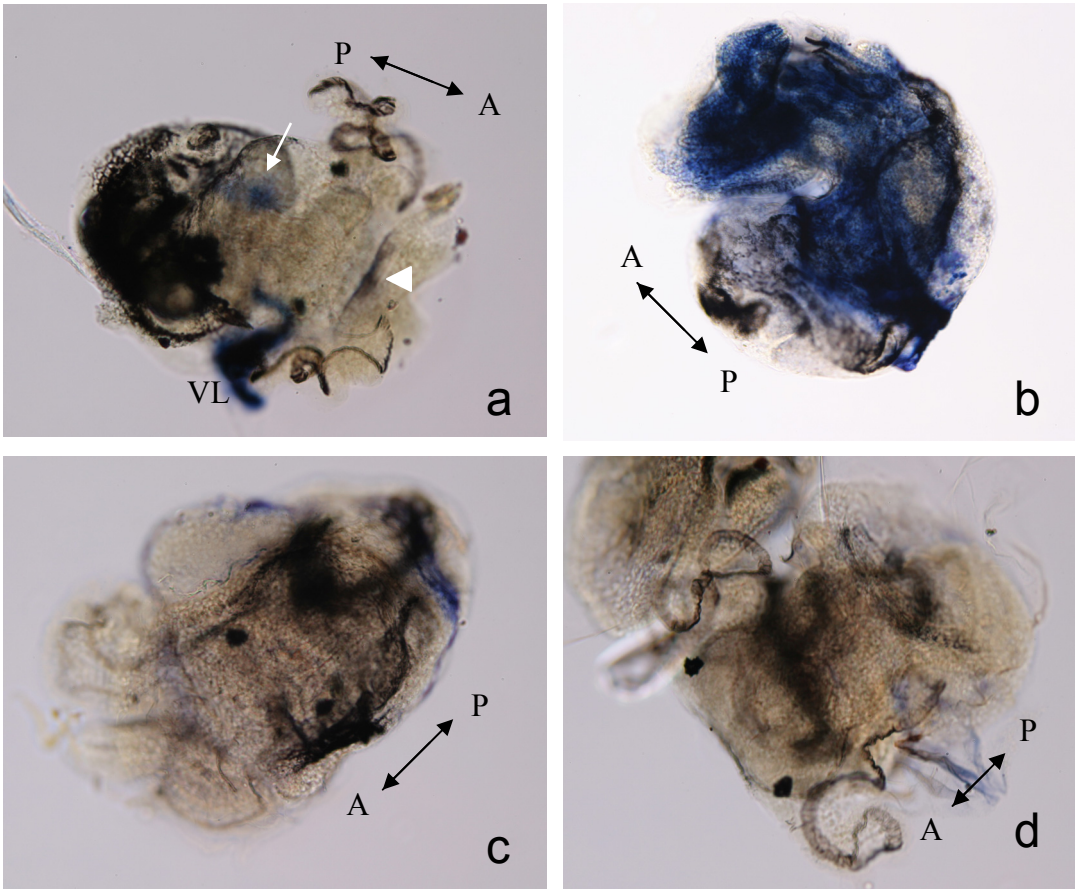

Figure 13. Localization of NOS mRNA by whole mount *in situ* hybridization. Competent larvae were fixed and probed with anti-sense NOS (a), anti-sense actin(b), sense NOS (c), or sense actin (d). NOS mRNA localization could be seen in the visceral mass (a, whitearrow), near the mouth (a, white arrow head) and on the edge of the velum (a, VL). Actin mRNA localization was found all over the body (b). A=anterior and P=posterior.

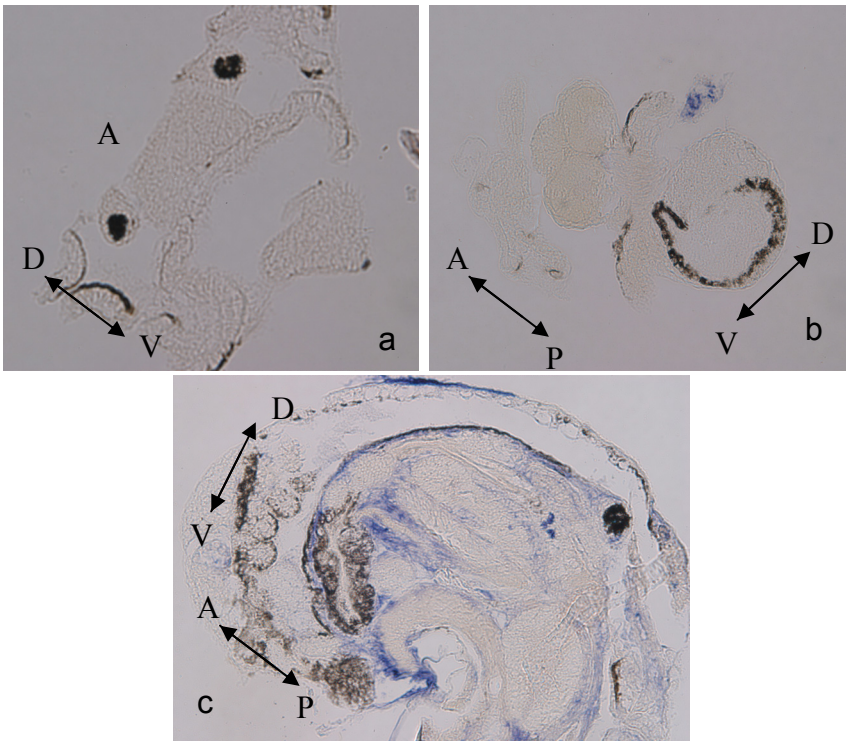

Figure 14. Localization of NOS mRNA in paraffin sections of larvae processed for whole mount *in situ* hybridization. Competent larvae were fixed, treated with an anti-sense NOS probe(a, b) or anti-sense actin (c), embedded in paraffin and sectioned at 10μm slices. Some NOS mRNA localization was seen in the visceral mass (b, white arrow) but none was seen in anterior sections near the location of the apical ganglion (a). A=anterior, P=posterior, D=dorsal, V=ventral.

CHAPTER IV

DISCUSSION

My results demonstrate the ability of the D4084-AP *Ilyanassa*-specific antibody to recognize *Ilyanassa* NOS protein in western blots. The NOS antibody allowed me to detect changes in NOS gene expression during development (Figures 8 and 10), and more importantly, during metamorphosis (Figures 9 and 11). These results agree with earlier studies of NOS expression levels (Hens *et al.,* 2006).

Production and characterization of *Ilyanassa*-specific NOS antibody

Serum selection and antigen recognition

The D4084 and D4085 sera detected the bacterially-produced GST-NOS fusion protein (Figure 4b). The expected size of the GST-NOS fusion protein was 38 kDa which can be seen in the stained gel (arrow in Figure 4a). The bands detected with the anti-NOS sera were at 35 kDa (Figure 4b; lanes 6 and 10). Although the 35 kDa band is not the predicted size, it is within the margin of error that is acceptable. In a study done by Weber and Osborn (1969), the size of proteins analyzed by SDS-PAGE can be predicted within ± 10% accuracy. This means that a 35 kDa protein is 31.5-38.5 kDa which is within an acceptable margin of error for the 38 kDa GST-NOS fusion protein. The NOS sera were unable to recognize products smaller than 35 kDa because polypeptides smaller than this would not contain the portion of the NOS to which this

antibody binds specifically. The smaller polypeptides of the GST-NOS fusion protein detected by the GST antibody at 33kDa and 28kDa (Figure 4b; lane 2) are likely to be degradation products of the protein. Protein degradation has been studied for many years and is a way for cells to eliminate harmful or malformed proteins (Goldberg and St. John, 1976). The larger protein that was detected by the NOS sera was not detected by the GST antibody probably because the quality of that product was less abundant.

The affinity purified D4084 antibody detected the GST-NOS fusion protein (Figure 5). Polypeptides detected were at 34 kDa, 36 kDa and 39 kDa (Figure 5; lane 2). The smaller polypeptides are likely to be degradation products. The prominent 39 kDa polypeptide is again within the margin of error for the full-size GST-NOS fusion protein.

These data demonstrate the ability for the *Ilyanassa*-specific NOS antibody to detect a portion of the *Ilyanassa* nNOS. Of greater importance was the ability of the NOS antibody to detect NOS in larval *Ilyanassa* and my use of the antibody as a tool to determine the temporal and spatial expression of NOS during metamorphosis in *Ilyanassa*.

D4084-AP was not only able to recognize the bacterially-produced NOS but showed specificity to nNOS epitopes in adult CNSs of *Ilyanassa* (Figure 7, lane 4). Polypetides at 176, 157, 102, 88 and 66 kDa showed immunoreactivity to the NOS antibody. When the NOS antibody was preabsorbed to the NOS peptide, polypeptides at 176, 157 and 66 kDa did not appear on the western blot. This demonstrates the specificity of D4084-AP to the 176, 157 and 66 kDa NOS polypeptides in *Ilyanassa*.

NOS immunoreactivity of Ilyanassa *proteins*

Nitric oxide synthase has been identified in a number of molluscs. For *Limax valentianus*, NOS has a deduced size of 180 kDa and for both *Sepia officinalis* and *Lymneae stagnalis,* the predicted size of NOS is 129 kDa (Matsuo *et al*., 2008; Scheinker *et al*., 2005; Korneev *et al*., 1997). For two other molluscan species, *Pleurobranchae californica* (Hurst *et al*., 1999) and *Aplysia californica* (GenBank accession# AAK83069), NOS has been determined to be 155 kDa and 153 kDa respectively. Based on these assumptions, it is reasonable to expect full size *Ilyanassa* NOS to be 129-180 kDa. Because *Aplysia californica* is of the same infraclass, Apogastropoda, as *Ilyanassa*, the most likely prediction is that *Ilyanassa* NOS is about 153 kDa. Although most of the size predictions of molluscan NOS have been deduced from predicted amino acid sequences, the predicted size of the protein in *Pleurobranchae* was determined by western blot analysis.

The affinity purified NOS antibody recognized polypeptides in larval extracts of 183 kDa, 116 kDa, 89 kDa and 66 kDa (Figure 6). There are many similarities between NOS bands in *Ilyanassa* and those reported for other molluscan species (Hurst *et al.*, 1999). In this study, mammalian neuronal NOS antibodies were used to probe western blots of CNSs from *Pleurobranchae californica*, *Aplysia californica* and *Tritonia diomedea*. Extracts from larval *Ilyanassa* display a band at 183 kDa which is comparable to the 200 kDa band seen in the CNS of *Tritonia*. The 116 kDa band in larval *Ilyanassa* is similar to bands in *Tritonia* ranging from 100-130 kDa. Both *Aplysia* and *Tritonia* exhibited an 85 kDa band much like the 89 kDa band seen in larval *Ilyanassa*. Finally,

the 66 kDa band from larval *Ilyanassa* is comparable to bands seen in *Aplysia* and *Tritonia* ranging from 60-70 kDa.

The affinity purified NOS antibody also detected multiple bands from adult CNSs of *Ilyanassa* at 176 kDa, 157 kDa, 102 kDa, 88kDa and 66kDa (Figure 7; lane 3) although the 102 kDa and 88 kDa bands were not still detected after pre-absorption with the NOS peptide antigen. Compared to the Hurst *et al.* (1999) study, adult CNSs of *Ilyanassa* display a band at 176 kDa which is comparable to the 200 kDa band seen in the CNS of *Tritonia*. In adult CNSs of *Ilyanassa*, a 157 kDa band is much like the 155 kDa band in the CNSs of *Pleurobranchae.* The 66 kDa band in adult CNSs of *Ilyanassa* is comparable to bands seen in *Aplysia* and *Tritonia* ranging from 70-60 kDa.

It is not surprising that *Ilyanassa* showed so many similarities in nNOS banding pattern with *Tritonia* as they are both members of the Apogastropoda infraclass. These similarities also speak to the somewhat predictable degradation products or possible isoforms of nNOS. Protein half-life can vary from minutes to weeks depending on the protein and protein degradation can happen as a result of lysosomal breakdown or in some cases by way of ubiquitination, in which protein are tagged with a small molecule called ubiquitin that allows the protein to be quickly broken down (Goldberg and St. John, 1976; Hershko and Ciechanover 1982). Other studies have shown evidence of ubiquination and proteosomal degradation of mammalian nNOS (Bender *et al*., 2000; Dunbar *et al*., 2004).

Another possible explanation for the various bands on western blots of larval *Ilyanassa* and adult CNSs is splice variants of nNOS. At least three splice variants of

nNOS have been studied in mammals (Eliasson *et al*., 1997; Huber *et al*., 1998). These splice variants code for proteins that range in size from 125 kDa to 150 kDa and vary in catalytic activity, the longest isoform having the most activity (Eliasson *et al*., 1997; Huber *et al*., 1998). Splice variants have also been studied in *Drosophila* and four variants have been identified that produce variously sized active or inactive proteins (Stasiv *et al*., 2001).

In the study by Hurst *et al*. (1999), no band was seen at 153 kDa, the expected size for nNOS based on amino acid prediction. This may be because NOS is easily degraded. However, a band of 157 kDa was seen in adult CNSs of *Ilyanassa* but is lacking in larval *Ilyanassa*. Furthermore, in preabsorption experiments with samples from adult CNSs of *Ilyanassa* (Figure 7; lane 4), the 157 kDa band disappeared, suggesting that this may a full length nNOS. A size of 176 kDa for full length nNOS must also be considered because this band also disappeared with preabsorption.

The 66 kDa band seen in both larval extracts and adult CNSs is interesting in that it occurs in all western blots of *Ilyanassa*. The binding of nNOS antibodies to lower molecular weight proteins may be evidence of degradation products of NOS or proteins related to NOS (Chen *et al*., 1997; Hurst *et al*., 1999). This may be a stable degradation product of nNOS because it was the most abundant in the adult CNS sample and disappeared in the preabsorption assay.

Determination of NOS protein levels during larval development and following induction of metamorphosis

NOS during larval development

An examination the 66 kDa band in western blots done to investigate the changes in temporal expression of NOS in larval *Ilyanassa* can give insight into possible changes in levels of full sized nNOS (Figures 8-11). Changes in optical density fluctuated during larval development (Figure 10). NOS levels at the onset of larval development, zero dph, are at their highest. As mentioned earlier, NO has many functions and this holds true even within an individual organism. For example, NOS is present in the CNSs of adult *Ilyanassa* (Figure 7) and is clearly not functioning in metamorphosis at this life history stage. At zero dph, NO may have another function such as modulating cell proliferation or axogenesis as it does in other invertebrates. In *Drosphila*, NO regulates cell proliferation and organization of retinal projections during eye development (Kuzin et al., 1996; Gibbs and Truman, 1998).

Between 7 and 11 dph NOS levels decrease and then rises at competency (18 dph). This is different from mRNA levels which stayed constant throughout larval development (Hens *et al.*, 2006). This could be due to post-translational regulation as proposed by Hens *et al.* (2006). My result also differ from Lin and Leise's (1996b) report of an increase in NADPH-diaphorase staining in the AG during larval development to the point of competency. NADPH-diaphorase was used as indication of the presence of NOS. However, NADPH-diaphorase staining only occurs when NOS is enzymatically active (Morris *et al*., 1997), which requires the presence of the cofactors NADPH,

calcium, calmodulin, THB and FAD (Huber *et al.,* 1998). In culture, FAD and calmodulin must be present for NOS activity to result in NADPH-diaporase staining (Morris *et al*., 1997). It is possible that the NOS that is present during larval development is not enzymatically active and thus does not produce NADPH-diaphorase staining. Even without an inducer present, larvae that are 28 dph may already be undergoing the beginnings of spontaneous metamorphosis. This process includes the programmed cell death of the AG and thus lowers NOS polypeptide levels (Gifondorwa and Leise, 2006). Decreased NOS enzyme activity and the resultant low NADPH-diaphorase activity have been demonstrated in brain tissue of rats. In this instance, NOS immunoreactivity occurred in both the posterior and anterior pituitary, but only the posterior pituitary showed NADPH-diaphorase staining (Wang *et al*., 1997).

NOS following induction of metamorphosis

Temporal expression of *Ilyanassa* NOS investigated by western blot analysis showed a decrease in NOS during metamorphosis (Figure 11), agreeing with earlier results from studies of mRNA levels and NADPH-diaphorase histochemistry (Hens et al., 2006; Lin and Leise, 1996b). These data all support the idea that a decrease in NOS enzymatic activity is due to a decrease in protein levels. They also support the idea that a decrease in NOS allows metamorphosis in *Ilyanassa* to occur.

Determination of spatial pattern of NOS gene expression

Results from successful *in situ* hybridization of *Ilyanassa* NOS would have been helpful in determining the spatial expression of NOS (Figures 13 and 14). As stated in the results, little hybridization could be seen using the anti-sense NOS probe. This may have been caused by the small size of the probe, 231 bp (Figure 12), that did not allow for proper hybridization. Successful hybridization usually requires a probe that is 200-500 bp (Jin *et al*., 1997; Dijkman *et al*., 1995). Small amounts of hybridization could be seen in the visceral mass of the larva (Figure 13a). This is consistant with Lin and Leise's (1996b) findings in which they saw some NADPH-diaphorse staining in the visceral mass in competent larvae. This hybridization may be the result of non-specific binding. Tharvaradhara and Leise (2001) saw non-specific NOS immunoreactivity in competent larvae. Because there was non-specific staining in larvae probed with sense probes, non-specific hybridization must be considered, although staining with sense probes usually only resulted in surface staining (Figure 13c and d). Even though hybridization of the NOS anti-sense probe could be seen in a variety of areas of the body, it varied between larvae and areas of hybridization was not reproducible. No hybridization was seen in the area of the apical ganglion despite more in depth visualization with tissue sectioning (Figure 14a and b).

The successful hybridization of the actin probe (Figure 13b) suggests that the protocol used was sufficient. However, actin is expected to be expressed in all of the cells and sections of the actin hybridized specimens showed spots of non-hybridization (Figure 14c). This suggests incomplete penetration of the probe due to the protocol used.

For these experiments I used a protocol optimized for *Xenopus* embryos because *in situ* hybridization is not commonly attempted in molluscs. Protocols used for other animals might help to optimize hybridization in *Ilyanassa.*

It is still uncertain exactly where NOS is located in the AG. Lin and Leise (1996b) observed NADPH-diaphorase staining in the neurophil of the AG but a mammalian nNOS antibody stained the cell bodies of the AG (Thavardhara and Leise, 2001). Attempts at immunohistochemistry assays with the *Ilyanassa*-specific NOS antibody resulted in no successful staining. This was likely due to less than optimal fixation or antibody incubation. More extensive optimization of these conditions could result in proper staining.

Conclusions

In summary, an *Ilyanassa*-specific NOS antibody was developed that recognizes the peptide against which it was developed, as well as various degradation products or isoforms of nNOS in larval *Ilyanassa* and adult CNSs. Use of this antibody demonstrated that NOS polypeptide levels fluctuate during larval development and decrease during metamorphosis. Differences in NOS mRNA evidence (Hens *et al*., 2006) as compared to my NOS protein data suggest post-transcriptional regulation. Evidence from NADPH-diaphorase histochemistry (Lin and Leise, 1996b) in comparison to my NOS protein data suggests that NOS may be inactive during parts of larval development, but becomes active during the competent phase to maintain the larval state until necessary metamorphic cues are encountered. Further experimentation needs to be done to

determine the location of NOS mRNA and protein in the AG and how the distribution of these change during larval development and metamorphosis.

REFERENCES

Alderton, W.K., Cooper, C.E., and Knowles, R.G. 2001. Nitric oxide synthase: structure function and inhibition. *Biochem. J.* **357:**593-615

Anderson, D.T. 2001. *Invertebrate Zoology*. Oxford University Press. 474pp

Bender, A.T., Demady, D.R., and Osawa, Y. 2000. Ubiquination of Neuronal Nitric-oxide Synthase in Vito and in Vivo. *The Journal of Biological Chemistry* **275:**17407-17411

Bishop, C.D., Bates, W.R. and Brandhorst, B.P. 2001. Regulation of Metamorphosis in Ascidians Involves NO/cGMP Signaling and HSP90. *Journal of Experimental Zoology* **289:**374-384

Bishop, C.D. and Brandhorst, B.P. 2001. NO/cGMP Signaling and HSP90 Activity Represses Metamorphosis in the Sea Urchin Lytechinus pictus. *Biol. Bull.* **201:**394-404

Boxshall, G.A. 2007. Crustacean classification: on-going controversies and unresolved problems. *Zootaxa* **1668:**313-325

Chen, D., Hurst, W.J., Ding, J.M., Faiman, L.E., Mayer, B. and Gillette, M.U. 1997. Localization and Characterization of Nitric Oxide Synthase in the Rat Suprachiasmatic Nucleus: Evidence for a Nitrergic Plexus in the Biological Clock. *Journal of Neurochemistry* **68:**855-861

Comes, S., Locascio, A. Silvestre, F., d'Ischia, M. and Palumbo, A. 2007. Regulatory roles of nitric oxide during larval development and metamorposis in Ciona intestinalis. *Developmental Biology* **306:**772-784

Couper, J.M. and Leise, E.M. 1996. Serotonin Injections Induce Metamorphosis in Larvae of the Gastropod Mollusc Ilyanassa obsoleta. *Biol. Bull*. **191:**178-186

Dawson, T.M., Bredt, D.S., Fotuni, M. Hwang, P.M. and Snyder, S.H. 1991. Nitric Oxide Synthase and neuronal NADPH diaphorase are identical in brain and peripheral tissues. *Proc. Natl. Acad. Sci. USA* **88:**7797-7801

Dawson, T.M. and Snyder, S.H. 1994. Gases as biological messengers: nitric oxide and carbon monoxide in the brain. *J. Neurosci*. **14:**5147-5159

Dickenson, A.J.G. and Croll, R.P. 2003. Development of the Larval Nervous System of the Gastropod Ilyanassa obsoleta. *Journal of Comparative Neurology* **466:** 197-218

Dijkman, H.B.P.M., Mentzel, S., de Jong, A.S., and Assmann, K.J.M. 1995. RNA In Situ Hybridization Using Digoxigenin-labeled cRNA Probes. *Biochemica* **2:**23-27

Dunbar, A.Y., Kamada, Y., Jenkins, G.J., Lowe, E.R., Billecke, S.S. and Osawa, Y. (2004) Ubiqitination and Degradation of Neuronal Nitric-oxide Synthase In Vito: Dimer Stabilization Protects the Enzyme from Proteolysis. *Mol. Pharmacol.* **66:**964-969

Eliasson, M.J., Blackshaw, S., Schell, M.J., and Synder, S.H. 1997. Neuronal nitric oxide synthase alternatively spliced forms: Prominent functional localizations in the brain. *Proc. Natl. Acad. Sci. USA* **94:**3396-3401.

Froggett, S.J. and Leise, E.M. 1999. Metamorphosis in the Marine Snail Ilyanassa obsoleta, Yes or NO? *Biol. Bull.* **196:**57-62

Fowler, K.A. 2005. Nitric Oxide Synthase Expression in the Nervous System of Competent and Metamorphosing Ilyanassa obsoleta*. Masters Thesis. The University of North Carolina at Greensboro.*

Gibbs, S.M. and Truman, J.W. 1998. Nitric Oxide and Cyclic GMP Regulate Retinal Patterning in the Optic Lope of Drosophila. *Neuron* **20:** 83-93

Gelperin, A. Flores, J. Raccuia-Behling, F. and Cooke, I.R. 2000. Nitric oxide and carbon monoxide oscillations of olfactory interneurons in terrestrial mollusk. *J. Neurophysiol.* **83:**116-127

Gharbiah, M., Cooley, J., Leise, E.M., Nakamoto, A., Rabinowitz, J.S. Lambert, J.D., and Nagy, L. 2008. Methods for studying development in the reemerging model spiralian Ilyanassa. *In Handbook of Non-Model Organisms*. Cold Spring Harbor Laboratory Press: Cold Spring Harbor, New York.

Gifondorwa, D.J. and Liese, E.M. 2006. Programmed Cell Death in the Apical Ganglion During Larval Metamorphosis of the Marine Mollusc Ilyanassa obsoleta. *Biol. Bull.* **210:**109-120

Goldberg, A.L. and St. John, A.C. 1976. Intracellular Protein Degradation In Mammalian and Bacterial Cells: Part 2. *Annu. Rev. Biochem.* **45:**747-804

Hadfield, M. 1998. The D P Wilson Lecture. Research on Settlement and Metamorphosis of Marine Invertebrate Larvae: Past, Present and Future. *Biofouling* **12:**9-29

Haszprunar, G. 2001. Mollusca (Molluscs). *Encyclopedia of Life Sciences* John Wiley and Sons, Ltd.

Hens, M.D., Fowler, K.A. and Leise, E.M. 2006. Induction of Metamorphosis Decreases Nitric Oxide Synthase Gene Expression in Larvae of the Marine Mollusc Ilyanassa obsoleta (Say). *Biol. Bull*. **211:**208-211

Hershko, A. and Ciechanover, A. 1982. Mechanisms of intercellular protein breakdown. *Annu. Rev. Biochem*. **51:**335-364

Hope, B.T., Michael, G.J., Knigge, K.M. and Vincent, S.R. 1991. Neuronal NADPH diaphorase is a nitric oxide synthase. *Proc. Natl. Acad. Sci. USA* **88:**2811-2814

Huber, A., Saur, D., Kurjak, M, Schusdziarra, V. and Allescher, H-D. 1998. Characterization and splice variants of neuronal nitric oxide synthase in rat small intestine. *Am. J. Physiol. Gastrointest. Liver Physiol.* **275:**1146-1156

Hurst, W.J., Moroz, L.L., Gillette, M.U. and Gillette, R. 1999. Nitric Oxide Synthase Imunolabeling in the Molluscan CNS and Peripheral Tissue. *Biochemical and Biophysical Research Communications* **262:**545-548

Jacklet, J.W. 1997. Nitric oxide signaling in invertebrates. *Invertebrate Neuroscience* **3:**1-14

Jin, L. and Llyod, R.V. 1997. In Situ Hybridization: Methods and Applications. *Journal of Clinical Laboratory Analysis* **11:**2-9

Korneev, S. and O'Shea, M. 2002. Evolution of Nitric Oxide Synthase Regulatory Genes by DNA Inversion. *Mol. Biol. Evol.* **19:**1228-1223

Korneev, S.A., Piper, M.R., Picot, J., Phillips, R., Korneeva, E.I. and O'Shea, M. 1998. Molecular Characterization of NOS in a Mollusc: Expression in a Giant Modulatory Neuron. *J. Neurobiol.* **35:**65-76

Kuzin, B., Roberts, I., Peunova, N., and Enikolopov, G. 1996. Nitric oxide regulates cell proliferation during Drosophila development. *Cell* **87:**639-649

Leise, E.M., Froggett, S.J., Nearhoof, J.E. and Cahoon, L.B. 2009. Diatom Culture Induce and Inhibit Larval Metamorphosis in the Marine Gastropod Ilyanassa obsoleta (Say). *Journal of Experimental Marine Biology and Ecology* (accepted)

Leise, E.M., Kempf, S.C., Durham, N.R. and Gifondorwa, D.J. 2004. Induction of metamorphosis in the marine gastropod Ilyanassa obsoleta: 5HT, NO and programmed cell death. *Acta Biologica Hungarica* **55:**293-300

Leise, E.M., Thavaradhara, K., Durham, N.R. and Turner, B.E. 2001. Serotonin and Nitric Oxide Regulate Metamorphosis in the Marine Snail Ilyanassa obsoleta. *Amer. Zool*. **41:**258-267

Levantine, P.L. and Bonar, D.B. 1986. Metamorphosis of Ilyanassa obsoleta: natural and artifical inducers. *Am. Zool.* **26:**14A

Lin, M-F. and Leise, E.M. 1996a. Gangliogenesis in the Prosobranch Gastropod Ilyanassa obsoleta. *The Journal of Comparative Neurology* **374:**180-193

Lin, M-F. and Leise, E.M. 1996b. NADPH-Diaphorase Activity Changes During Gangliogenesis and Metamorphosis in the Gastropod Mollusc Ilyanassa obsoleta. *The Journal of Comparative Neurology* **374:**194-203

Matsuo, R., Misawa, K. and Ito, E. 2008. Genomic structure of nitric oxide synthase in the terrestrial slug is highly conserved. *Gene* **415:**74-81

Miller, S.E. and Hadfield, M.G. 1986. Ontogeny of phototaxis and metamorphic competence in larvae of the nudibranch Phestilla sibogae Bergh (Gastropoda Opisthobranchia). *J. Exp. Mar. Biol. Ecol*. **97:**95-112

Morris, B.J., Simpson, C.S., Mundell, S., Maceachern, K., Johnston, H.M., and Nolan, A.M. 1997. Dynamic Changes in NADPH-diaphorase Staining Reflect Activity of Nitric Oxide Synthase: Evidence for a Dopaminergic Regulation of Striatal Nitric Oxide Release. *Neuropharmacology* **36:**1589-1599

Morse, A.N.C. and Morse, D.E. 1984. Recruitment and metamorphosis of Haliotis larvae induced by molecules uniquely available at the surface of crustose red algae. *J. Exp. Mar. Biol. Ecol.* **75:**191-215

Morse, D.E. 1979. γ-Aminobutyric Acid, a Neurotransmitter, Induces Plantonic Abalone Larvae to Settle and Begin Metamorphosis. *Science* **204:**407-410

Morse, D. E. 1985. Neurotransmitter-mimetic inducers of larval settlement and metamorphosis. *Bull. Mar. Sci.* **37:** 697-706

Novas, A., Barcia, R., and Ramos-Martinez, J.I. 2007. After the Prestige oil spill modifications in NO production and other parameters related to the immune response were detected in hymocytes of Mytilus galloprovincialis. *Aquatic Toxicology* **85:**285-290

Palumbo, A. 2005. Nitric oxide in marine invertebrates: A comparative perspective. *Comparative Biochemistry and Physiology, Part A* **142:**241-248

Pawlik, J.R. 1992. Induction of Marine Invertebrate Larval Settlement: Evidence for Chemical Cues. *Ecological Roles of Marine Natural Products.* Cornell University Press: Ithaca, NY

Pechenik, J.A., Cochrane, D.E., Li, W., West, E.T., Pires, A. and Leppo, M. 2007. Nitric Oxide Inhibits Metamorphosis in Larvae of Crepidula formicata, the Slippershell Snail. *Biol. Bull*. **213:**160-171

Peunova, N., Kuzin, B., Roberts, I., O'Kane, C., and Enikolopov, G. 1996. Nitric Oxide, Cell Multiplication and Cell Survival. *Cold Springs Harbor Symposia on Quantitative Biology* **61:**417-426

Pires, A., Croll, R.P., and Hadfield, M.G. 2000. Catecholamines Modulate Metamorphosis in the Opisthobranch Gastropod Phestilla sibogae. *Biol. Bull*. **198:**319-331

Presnell, J.K. and Schreibman, M.P. 1997. *Humason's Animal Tissue Techniques, Fifth Edition.* The John Hopkins University Press: Baltimore, MD p. 469

Regulski, M. and Tully, T. 1995. Molecular and biochemical characterization of dNOS: a Drosophila Ca2+/ Calmodulin-dependant nitric oxide synthase. *Proc. Natl. Acad. Sci. USA* **92:**9072-9076

Scheinker, V., Fiore, G., Di Cristo, C., Di Cosmo, A. d'Ischia, M., Enikolopov, G. and Palumbo, A. 2005. Nitric oxide synthase in the nervous system and ink gland of the cuttlefish Sepia officianlis: Molecular cloning and expression. *Biochemical and Biophysical Research Communications* **338:**1204-1215

Scheltema, R.S., 1961. Metamorphosis of the veliger larvae of Nassarius obsoletus (Gastropoda) in response to bottom sediment. *Biol. Bull.* **120:** 92-109

Scheltema, R.S. 1962. Pelagic larvae of New England intertidal gastropods I. Nassarius obsoletus Say and Nassarius vibex Say. *Transactions of American Microscopial Society* **81:**1-11

Stasiv, Y., Regulski, M., Kuzin, B., Tully, T., and Enikolopov, G. 2001. The Drosophila Nitric-oxide Synthase Gene (dNOS) Encodes a Family of Proteins That Can Modulate NOS Activity by Acting as Dominant Negative Regulators. *The Journal of Biological Chemistry* **276:**42241-42251

Thavaradhara, K. and Leise, E.M. 2001. Localization of nitric oxide synthase-like immunoreactivity in the developing nervous system of the snail Ilyanassa obsoleta. *Journal of Neurocytology* **30:**449-456

Trapido-Rosenthal, H.G. and Morse, D.E. 1986. Regulation of Receptor-mediated Settlement and Metamorphosis in larvae of a Gastropod mollusc (Haliotis Rufescens). *Bulletin of Marine Science* **39:**383-392

Wang, H., Christian, H.C., Morris, J.F. 1997. Dissociation of nitric oxide synthase immunoreactivity and NADPH-diaphorase enzyme activity in rat pituitary. *Journal of Endocrinology* **154:**R7-R11.

Weber, K. and Osborn, M. 1969. The Reliability of Molecular Determinations by Dodecyl Sulfate-Polyacrylamide Gel Electrophoresis. *The Journal of Biological Chemistry* **244:**4406-4412

Yu, X., He, W., Gu, J-D., He, M., and Yan, Y. 2008. The effect of chemical cues on settlement of pearl oyster Pinctada fucata martensii (Dunker) larvae. *Aquaculture* **277:** 83-91

Yvin, J.C., Chevolot-Magueur, A.M., and Cochard, J.C. 1985. First Isolation of jacaranone from an alga, Delesseria sanguinea. A metamorphic inducer of Pecten larvae. *J. Nat. Prod.* **48:**814-816

Zimmer-Faust, R.K. and Tamburri, M.N. 1994. Chemical identity and ecological implications of a waterbourne, larval settlement cue. *Limnol. Ocenaogr.* **39:**1075-1087